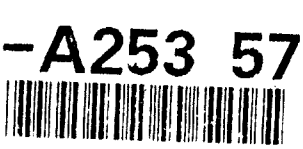

COLUMBIA UNIVERSITY

MICROELECTRONICS SCIENCES LABORATORIES

FINAL REPORT

to the

OFFICE OF NAVAL RESEARCH
UNIVERSITY RESEARCH INITIATIVE PROGRAM

INTERFACIAL AND THIN FILM CHEMISTRY IN ELECTRON DEVICE FABRICATION

Contract N00014-86-K-0694
for the period
September 15, 1986 - December 31, 1991

Columbia University in the City of New York

New York, New York 10027

January 1992

SECURITY CLASSIFICATION OF THIS PAGE

REPORT DOCUMENTATION PAGE

Form Approved
OMB No 0704-0188

1a REPORT SECURITY CLASSIFICATION unclassified	1b RESTRICTIVE MARKINGS NONE
2a SECURITY CLASSIFICATION AUTHORITY	3 DISTRIBUTION / AVAILABILITY OF REPORT Approved for public release; distribution unlimited
2b DECLASSIFICATION / DOWNGRADING SCHEDULE	
4 PERFORMING ORGANIZATION REPORT NUMBER(S)	5 MONITORING ORGANIZATION REPORT NUMBER(S)
6a NAME OF PERFORMING ORGANIZATION Columbia University Microelectronics Sciences Labs 6b OFFICE SYMBOL (If applicable)	7a NAME OF MONITORING ORGANIZATION Office of Naval Research
6c ADDRESS (City, State, and ZIP Code) Columbia University Microelectronics Sciences Laboratories 500 West 120th St., New York, NY 10027	7b ADDRESS (City, State, and ZIP Code) Arlington, VA 22217-5000
8a NAME OF FUNDING / SPONSORING ORGANIZATION ONR/URI 8b OFFICE SYMBOL (If applicable) Code 1114	9 PROCUREMENT INSTRUMENT IDENTIFICATION NUMBER N00014-86-K-0694
8c ADDRESS (City, State, and ZIP Code) Office of Naval Research 800 North Quincy Street Arlington, VA 22217-5000	10 SOURCE OF FUNDING NUMBERS PROGRAM ELEMENT NO: 61153N PROJECT NO: TASK NO: WORK UNIT ACCESSION NO:

11 TITLE (Include Security Classification)
FINAL REPORT: INTERFACIAL AND THIN FILM CHEMISTRY IN ELECTRON DEVICE FABRICATION

12 PERSONAL AUTHOR(S) Professors D. Auston, G. Flynn, I. Herman, R. Osgood, N. Turro, W. Wang, and E. Yang

13a TYPE OF REPORT	13b TIME COVERED	14 DATE OF REPORT (Year, Month, Day)	15 PAGE COUNT
Final Report	FROM 09/15/86 TO 12/31/91	January 1992	67 pages

16 SUPPLEMENTARY NOTATION

17 COSATI CODES			18 SUBJECT TERMS (Continue on reverse if necessary and identify by block number)
FIELD	GROUP	SUB-GROUP	See reverse side.

19 ABSTRACT (Continue on reverse if necessary and identify by block number)

Progress on the Columbia URI program on INTERFACIAL AND THIN FILM CHEMISTRY IN ELECTRON DEVICE FABRICATION is reported for the 1986-1991 period. Three broad areas of research included MBE Growth and Devices, Laser Surface Interactions, and Fundamentals of Processing Gas/Surface Interactions. Research in the area of MBE Growth and Devices included "Heterostructures Grown by Molecular Beam Epitaxy" by Professor Wen Wang and "Interface Chemical Modification of Metal on Superconductor-Semiconductor Systems" by Professor Ed Yang. Research in the area of Laser Surface Interactions included "Laser-Surface Interactions and *In Situ* Diagnostics of Surface Chemistry During Electronic Processing" by Professor Richard Osgood, Jr.; "*In Situ* Optical Diagnostics of Semiconductors Prepared by Laser Chemical Processing and Other Novel Methods" by Professor Irving Herman; and "Ultrafast Optoelectronic Measurements of Surfaces and Interfaces" by Professor David Auston. Research in Fundamentals of Processing Gas/Surface Interactions included "Quantum State-Resolved Studies of Gas/Surface Chemical Reactions" by Professor George Flynn and "Photochemical and Photophysical Probes of Interfaces" by Professor Nicholas Turro. Research results of Columbia's Principal Investigators supported by ONR/URI were published in nearly 200 scholarly articles which are listed in this report.

20 DISTRIBUTION / AVAILABILITY OF ABSTRACT ☒ UNCLASSIFIED/UNLIMITED ☐ SAME AS RPT ☐ DTIC USERS	21 ABSTRACT SECURITY CLASSIFICATION Unclassified
22a NAME OF RESPONSIBLE INDIVIDUAL Professors George Flynn and Richard Osgood	22b TELEPHONE (Include Area Code) 212-854-3265 22c OFFICE SYMBOL MSL

DD Form 1473, JUN 86 *Previous editions are obsolete*

SECURITY CLASSIFICATION OF THIS PAGE

SUBJECT TERMS (Block 18 Report Documentation Page)

molecular beam epitaxy
strain
tunneling
chlorine atoms
chemical reactions
cold rotations
diode lasers
excimer lasers
electrons
collision dynamics
electron scattering
surfaces
bronsted acids
zeolites
chemically induced dynamic nuclear polarization (CIDNP)
photopolymerization initiators
oxides in GaAs
GaAs
plasma screening
SEED devices
metal alkyls
surface diagnostics
$(CH_3)_3Ga$
SiC
High Tc-superconductors
HBT's
laser-assisted etching
copper
copper chloride
Raman scattering
silicon
germanium
strained layer superlattice
hydrostatic pressure
germanium-silicon alloy
heterostructures
optical modulators
charge coupled devices
Cl, D_2S, DCl, C_6D_{12}, S_2Cl_2
transition state
hot vibrations
GaAs CCD
2DEG CCD
resistive gate
dark current
InGaAs CCD
buried-channel CCD

ONR FINAL REPORT

I. TECHNICAL SUMMARIES

A. MBE GROWTH AND DEVICES

1. Heterostructures Grown by Molecular Beam Epitaxy (W. Wang)

a. First Integration of a Modulation-doped FET and a Resonant Tunneling Diode: We demonstrated the first integration of a modulation-doped FET and a resonant tunneling diode, which we called "A Two-dimensional Electron Gas Modulated Resonant Tunneling Transistor." Three-terminal resonant tunneling devices have been explored in the hope of exploiting the high speed of the tunneling process and the increased function of a device which exhibits a bi-stable input or output characteristic. To date resonant tunneling structures have been incorporated into a wide variety of transistor structures, but unfortunately the ultimate operating speed of those proposed devices is not close to that of the resonant tunneling process because the speed is limited by the FET or HBT structure in which the device is incorporated. In this context, we have demonstrated the operation of a novel three-terminal resonant tunneling device that operates on a principle fundamentally different from those previously proposed and which has the potential for operation speeds close to that of a discrete resonant tunneling diode. The device called a two-dimensional electron gas modulated resonant tunneling transistor consists of an AlGaAs/GaAs (planar) modulation-doped structure grown on top of an AlAs/GaAs double-barrier resonant tunneling heterostructure. Resonant tunneling transport between the source and drain is controlled by the drain-to-source voltage while the gate voltage controls the number of carriers available for the tunneling process by modulating the density of carriers in a two-dimensional electron gas. Since the drain-to-source transit time is essentially the tunneling time, high speed operation is limited by the RC time constants associated with the gate and the resonant tunneling diode portion of the device. In an optimized device structure and process, these time constants can be minimized to yield operation speeds well into the hundred gigahertz range, which would be only a factor of 2

or 3 lower than the speed associated with the resonant tunneling diode. In addition to high operation speeds, many of the complex analog and digital circuit functions realized by the other resonant tunneling transistors are possible with this device, such as a microwave power oscillator and single transistor flip-flop.

b. Existence of Internal Piezoelectric Fields in GaInSb/InAs Strained Layer Superlattices: We demonstrated by optical induced femtosecond electromagnetic pulses the existence of the internal piezoelectric fields in GaInSb/InAs strained layer superlattices for the first time (in collaboration with D. H. Auston). Theoretical studies have indicated that strained-layer multi-quantum wells grown in the (N11) axis exhibit large built-in electric fields that arise from the piezoelectric effect, while those grown on (100) substrate will not. We have demonstrated for the first time the equal strength but opposite direction of strained-induced piezoelectric fields for GaInSn/InAs superlattices grown in (311)A and (311)B orientations. Previously under this program, in collaboration with Dr. Ben Shanabrook *et al.* of NRL, we have demonstrated the screening of the internal piezoelectric field in (111)B GaSb/AlSb strained multilayer structures by optically generated free carriers, which is the principle for optically-controlled optical switch. The present work confirmed that the electric fields associated with A- and B- face have opposite directions, as predicted by D.L. Smith of Livermore Laboratory.

c. Growth of High Quality GaAs Single Quantum Wells: We demonstrated the growth of high quality GaAs single quantum wells at low temperature by modulated beam epitaxy. High quality AlGaAs/GaAs quantum wells have been successfully grown at low temperatures (500 °C) by a modulated beam epitaxy process in which the Group III flux is held constant while the Group V (As) flux is periodically shut off to produce a metal-rich surface. The low temperature photoluminescence (PL) of single quantum wells grown with this technique exhibit full-width at half maximum values comparable to the best attainable by higher temperature growth techniques. The narrowness of the observed PL spectra is attributed to a smoothing of the growth front and a

reduction of excess As during the modulated beam epitaxy growth process. Both of these improvements are a result of the metal-rich condition which is produced when the As is shut-off in modulated beam epitaxy process. Under metal-rich conditions, both the metal migration on the surface and As incorporation are enhanced over the normal As rich growth condition. The ability of this technique to rapidly smooth an unreconstructed substrate surface was directly observed by monitoring reflection high energy diffraction patterns during standard MBE and modulated beam epitaxial growth. GaAs quantum well lasers grown with this technique exhibit the lowest threshold current densities (<1kA/cm^2) of any low temperature grown device, and further confirm the ability of this technique to produce high quality AlGaAs layers and GaAs quantum wells at low growth temperatures. The high growth rates of the modulated beam epitaxy process make this technique a more attractive alternative than migration enhanced epitaxy and other growth interruption techniques for the low temperature growth of high quality quantum well structures.

d. Low Temperature Growth of GaAs Quantum Well Lasers by Modulated Beam Epitaxy:

GaAs single quantum well lasers have been successfully grown at low temperatures (500° C) by a modulated beam epitaxy process in which the Al/Ga flux is held constant while the As flux is periodically shut off to produce a metal-rich surface. The threshold current densities (<1kA/cm^2) of lasers grown by this technique are lower than normally grown low temperature lasers and are the lowest achieved by any low substrate temperature growth technique. The improvement in threshold current density is attributed to both an improved inverted quantum well interface and a reduction in excess As related defects. Improvement of the inverted quantum well interface (i.e., GaAs on top of AlGaAs) is a result of the metal-rich condition created when the As shutter is closed. Under metal-rich conditions the surface mobility of group III adatoms is enhanced producing a smoother growth front. Furthermore, a Ga-rich surface takes up As much more efficiently than a borderline Ga-rich surface. Therefore, the modulated beam epitaxy process allows the low temperature growth of AlGaAs layers at a lower total As flux than is typically possible in a normal MBE growth process. As a result, the amount of excess As, which are often

associated with non-radiative recombination centers, is reduced by the modulated beam epitaxy process. Furthermore, this modulated beam epitaxy process is a more practical alternative for the growth of laser structures than migration enhanced epitaxy due to its high growth rate, less frequent shutter operation and less background impurity incorporation (no growth interruptions).

e. MBE Growth of High Mobility GaSb and Pin Diode with High Breakdown Voltage: The *p*-type nature of unintentionally doped GaSb molecular beam epitaxy grown layers has been attributed to native defects resulting from insufficient Sb incorporation. Since the (111)B orientation provides the most Sb-rich environment for GaSb epilayer growth, it should result in fewer defects associated with the deficiency of Sb. We have grown GaSb pin diode structures on (111)B GaSb and found that the breakdown voltages are consistently higher than those grown on (100) substrates side-by-side. In addition, since the growth on the (111) orientation is in general much more difficult than (100), we propose that the (311)B orientation provides more optimal growth conditions for GaSb since the (311)B orientation still retains 50% of the (111)B-like Sb-rich character, and it also supports a (100)-like monolayer growth mode which is less plagued with defects than (111) growth. To support this claim, growth on (311)B substrates was studied and shown to produce Te-doped GaSb layers with room temperature mobilities of 6780 $cm^2/V\text{-}s$ at carrier densities of $9x10^{15}$ cm^{-3} and AlGaSb/GaSb *p-i-n* diode structures with breakdown voltages as high as 20 V. This n-type mobility is an improvement over that reported by Chen and Cho [JAP **70** , 277 (1991)], 5114 $cm^2/V\text{-}s$ at a carrier density of $3.8x10^{16}$ cm^{-3}, and presently represents the highest value achieved for molecular beam epitaxy grown GaSb. Presumably, the high mobilities and high breakdown voltages achieved are due to a reduction of native acceptor-type defects and can be improved in the future through further refinement of the growth process.

f. Photo-Hall Studies of High Purity GaAs Grown by Molecular Beam Epitaxy: We have grown high purity GaAs that exhibits liquid nitrogen mobility of 180,000 $cm^2/V\text{-}sec$ and a peak mobility of 300,000 $cm^2/V\text{-}sec$ at 45K at a layer thickness as thin as 11 um. Due to the significant

electron trapping by surface and interface states at low temperatures, the epitaxial layer becomes semi-insulating which is difficult to characterize. To facilitate the electrical measurements, at 4.2 K, the sample is momentarily illuminated by above bandgap light, which causes a reduction in surface and interface depletion region. After illumination, the effect of photoinduced charge neutral region persists until, at some higher temperature, the charge distribution in the sample relaxes back to its original equilibrium state. Results of variable temperature Hall measurements (in collaboration with Dr. M. H. Kim, Bandgap Technology, Inc., and G. E. Stillman, Univ. of Illinois), performed under these conditions, show that the sheet concentration is increased as compared to measurements obtained in the dark, but that mobility is unchanged. The increase in sheet carrier concentration after illumination results from the decrease of the surface and interface depletion widths. Such measurements can provide a method for judging the quality of layers that are fully depleted of free carriers at low temperature in the dark. These results are published in J. Applied Physics **70**, 7425 (1991).

g. P-type Doping of Molecular Beam Epitaxy (MBE) Grown GaSb by Ge and Sn: We demonstrated P-type doping of molecular beam epitaxy (MBE) grown GaSb by Ge and Sn for the first time. Both impurities are well behaved with demonstrated free acceptor concentrations as high as $2x10^{19}$ cm^{-3} for Ge and $5x10^{18}$ cm^{-3} for Sn. In addition, reflection high-energy electron diffraction (RHEED) measurements during growth indicate that Sn segregation, which is common in GaAs, does not occur in GaSb. The absence of Sn segregation as well as the p-type nature of Ge and Sn dopants is attributed to the large covalent bond radius of Sb. These dopants are important since they provide an excellent alternative to Be for p-type doping of Sb based materials.

2. Interface Chemical Modification of Metal on Superconductor-Semiconductor Systems (E. Yang)

a. GaAs Surfaces and Schottky Barriers: We have studied the gallium arsenide surfaces by exposing them to ultraviolet light and found enhanced reaction with oxygen.[1] Making use of UV-grown oxide, we have fabricated Schottky barriers with a barrier height strongly dependent on the interface oxide layer.[2] It was found that the GaAs surface can be chemically modified to bring about the control of the Schottky barrier.[3] Oxidation appears to shift the surface states toward the band edges allowing a wider range of Fermi level movements.[4] Thus, the altered interface chemistry is shown to be important for Schottky barrier formation. The dependence of the deep-level ELZ on the Schottky barrier height was measured by DLTS.[5]

b. High Temperature Superconducting (HTCS) Film on Silicon: Superconducting YBaCuO films have been formed by rapid thermal annealing of a multi-layered structure on MgO, with a zero resistance temperature at 84K.[6] Similar results were obtained for YBaCuO on SiO_2.[7] With the same process on silicon, silicon was found to diffuse throughout the superconducting film, and it destroyed the superconductivity.[8] The inhibition of superconductivity, because of Si-YBaCuO intermixing was found to be useful to form patterns of HTCS with a line width as narrow as 2.5 μm.[9,10] The method of patterning eliminates the need for chemical processing and is now known as reaction patterning. A patent was issued to Columbia in Dec. 1991.[11] With the ability to fabricate line structures, we produced a current controlled HTCS switch using the critical current as the reference for switching.[12] Some logic circuits were also proposed.

A key issue of practical importance is the ohmic contact between HTCS and normal metal. We have studied the interface chemistry and resistance at Metal-HTCS contacts. Although Au, Pt and Pd have similar contact resistivity at room temperature, only Au contact experiences a large decrease in contact resistance at 77K.[13] For other metals with high contact resistance, a thin

interface Au layer of 10Å is sufficient to bring it down by 2-3 order of magnitude.[14] Application of this technique to Nb/Au, Al/Au and Cu/Au bimetal contacts were also completed.[15-17]

A large resistive transition between 160-200K had been observed in $Y_5Ba_6Cu_{11}O_x$ films.[16]

c. Optically Induced Electromagnetic Radiation From Semiconductor Surfaces: Ultrafast electromagnetic radiation induced by a femtosecond laser beam from a semiconductor provides determination of the impurity doping concentration, carrier mobility, sign, and strength of the depletion field near the semiconductor surface.[18]

d. AlGaAs/GaAs Heterojunction Bipolar Transistors:[19] We fabricated the first two-dimensional electron gas (2-DEG) emitter heterojunction bipolar transistor. This device, which was grown by molecular beam epitaxy, incorporates an undoped GaAs spacer between the emitter and base of a standard AlGaAs/GaAs single-heterojunction bipolar transistor. The introduction of the spacer layer causes the formation of a 2-DEG at the AlGaAs/GaAs interface. This 2-DEG defines the emitter side of the junction and produces an emitter-base characteristic similar to that of the collector GaAs homojunction. Using a 300 Å GaAs spacer, offset voltages as low as 30 mV have been attained. These devices also exhibit current gains greater than 10 at emitter current densities of 3 A/cm^2 and gains up to 400 in the high current density regime.

We performed the first experiment of Electron Cyclotron Resonance (ERC) hydrogen (H) and nitrogen (N) plasma surface passivation on the AlGaAs/GaAs heterojunction bipolar transistor (HBT).[20] As a result of the plasma processing, the base current ideality factor was improved from 2.67 to 1.96, and the maximum current gain was increased from 720 to 1000. In the low current regime, the base current was reduced by two orders of magnitude. The nitride layer grown by nitrogen plasma passivates the GaAs surface and is stable for weeks without degradation.

References:

1. C. F. Yu, M. T. Schmidt, D. V. Podlesnik, E. S. Yang, and R. M. Osgood, Jr., J. Vac. Sci. Technol. A **6**, 754 (1988).

2. M. T. Schmidt, D. V. Podlesnik, C. F. Yu, X. Wu, R. M. Osgood, Jr., and E. S. Yang, J. Vac. Sci. Technol. B **6**, 1436 (1988).

3. M. T. Schmidt, D. V. Podlesnik, H. L. Evans, C. F. Yu, E. S. Yang, and R. M. Osgood, Jr., J. Vac. Sci. Technol. A **6**, 1446 (1988).

4. M. T. Schmidt, Q. Y. Ma, D. V. Podlesnik, R. M. Osgood, and E. S. Yang, J. Vac. Sci. Technol. B **7**, 980 (1989).

5. Q. Y. Ma, M. T. Schmidt, X. Wu, H. L. Evans, and E. S. Yang, J. Appl. Phys. **64**, 2469 (1988).

6. Q. Y. Ma, T. J. Licata, X. Wu, and E. S. Yang, Appl. Phys. Lett. **53**, 2229 (1988).

7. Q. Y. Ma, E. S. Yang amd C.-A. Chang, J. Appl. Phys. **66**, 1866 (1989).

8. Q. Y. Ma, X. Wu, M. T. Schmidt, E. S. Yang, and C.-A. Chang, Physica C **162**, 637 (1989).

9. Q. Y. Ma, E. S. Yang, G. V. Treyz, and C.-A. Chang, Appl. Phys. Lett. **55**, 896 (1989).

10. Q. Y. Ma, E. S. Yang, G. V. Treyz, C. Shu, R. M. Osgood, Jr., and C.-A. Chang, Mat. Res. Soc. Symp. Proc. **169**, 1189 (1990).

11. Personal correspondence dated December 19, 1991, from F. Kant, Columbia University Office of Science and Technology Development, to E. S. Yang and Q. Ma, regarding US Patent: "Method of Patterning Superconducting..."

12. Q. Y. Ma and E. S. Yang, Cryogenics **30**, 1146 (1990).

13. M. T. Schmidt, Q. Y. Ma, L. S. Weinman, X. Wu, E. S. Yang, and C.-A. Chang, American Institute of Physics, 218 (1990).

14. Q. Y. Ma, M. T. Schmidt, L. S. Weinman, E. S. Yang, S. M. Sampere and S.-W. Chan, J. Vac. Sci. Technol. A **9**, 390 (1991).

15. Q. Y. Ma, M. T. Schmidt, L. S. Weinman, E. S. Yang, S. M. Sampere and S.-W. Chan, Proc. of the APS **36**, 887 (1991).

16. Q. Y. Ma, C.-A. Chang, and E. S. Yang, J. Appl. Phys. **69**, 7348 (1991).

17. Q. Y. Ma, M. T. Schmidt, E. S. Yang, S.-W. Chan, D. Bhattachayra, J. P. Zheng and H. S. Kwok, preprint submitted to Appl. Phys. Lett., October 1991.

18. X.-C. Zhang, J. T. Darrow, B. B. Hu, D. H. Auston, M. T. Schmidt, P. Tham, and E. S. Yang, Appl. Phys. Lett. **56**, 2228 (1990).

19. Q. Wang, Y. Wang, K. F. Longenbach, E. S. Yang and W. I. Wang, Appl. Phys. Lett. **59**, 2582 (1991).

20. Q. Wang, E. S. Yang, P.-W. Li, Z. Lu, R. M. Osgood, Jr., and W. I. Wang, IEEE Electron Dev. Lett. **13**, 83 (1992).

B. LASER SURFACE INTERACTIONS

1. Laser and Atom Surface Interactions and *In Situ* Diagnostics of Surface Chemistry During Electronic Processing (R. Osgood)

During this final year, our research program has concentrated on ECR plasma and oxidation, and oxidation removal (surface cleaning) of GaAs, GaSb, and InAs. In the first investigation, we have used UHV diagnostics in the form of high resolution XPS and LEED to study the chemistry of oxidation and reactive surface cleaning by an ECR plasma source (Dr. William Holber at IBM). Important portions of the work have been done in collaboration with Professors Yang and Wang and their students. The investigation has had three major successes: 1) the development of a specific low temperature procedure for oxide removal and restored surface crystallinity for GaAs; 2) the first demonstration of the use of ECR plasma surface preparation for GaSb; and 3) the demonstration of the applicability of this technique for the improvement of device operation for devices made of GaAs and GaSb. In addition, our work has emphasized obtaining a fundamental understanding of the associated surface chemistry on the semiconductor surface. Thus, we have measured shifts in the valence state of the oxide with temperature as well as its temperature dependent shift in composition.

The application and removal of surface oxide of compound semiconductors has several important near term applications. First, GaAs oxides are being used with increasing frequency for *in situ* masking during patterning of GaAs-based materials; second, *in situ* oxides for an important intentional or coincidental capping structure which must be removed prior to MBE or MOCVD growth. The removal must be done at low temperatures and without pitting or damaging the crystallinity of the substrate surface.

The surface chemistry of GaAs-oxide removal with electron cyclotron resonance (ECR) hydrogen plasma has been investigated with monochromatic X-ray photoelectron spectroscopy (MXPS).[1] It was found that As-oxide is efficiently removed at room temperature, and heating expedited the removal of Ga-oxide (see Fig. 1). Band bending change, which correlates with the

surface state density changes during ECR hydrogen-plasma oxide reduction, was also observed (Fig. 2). This type of band bending change could well be responsible for hydrogen plasma passivation effects on many GaAs based devices including the significant passivation effect on GaAs/AlGaAs heterojunction bipolar transistor[2] as we will discuss later.

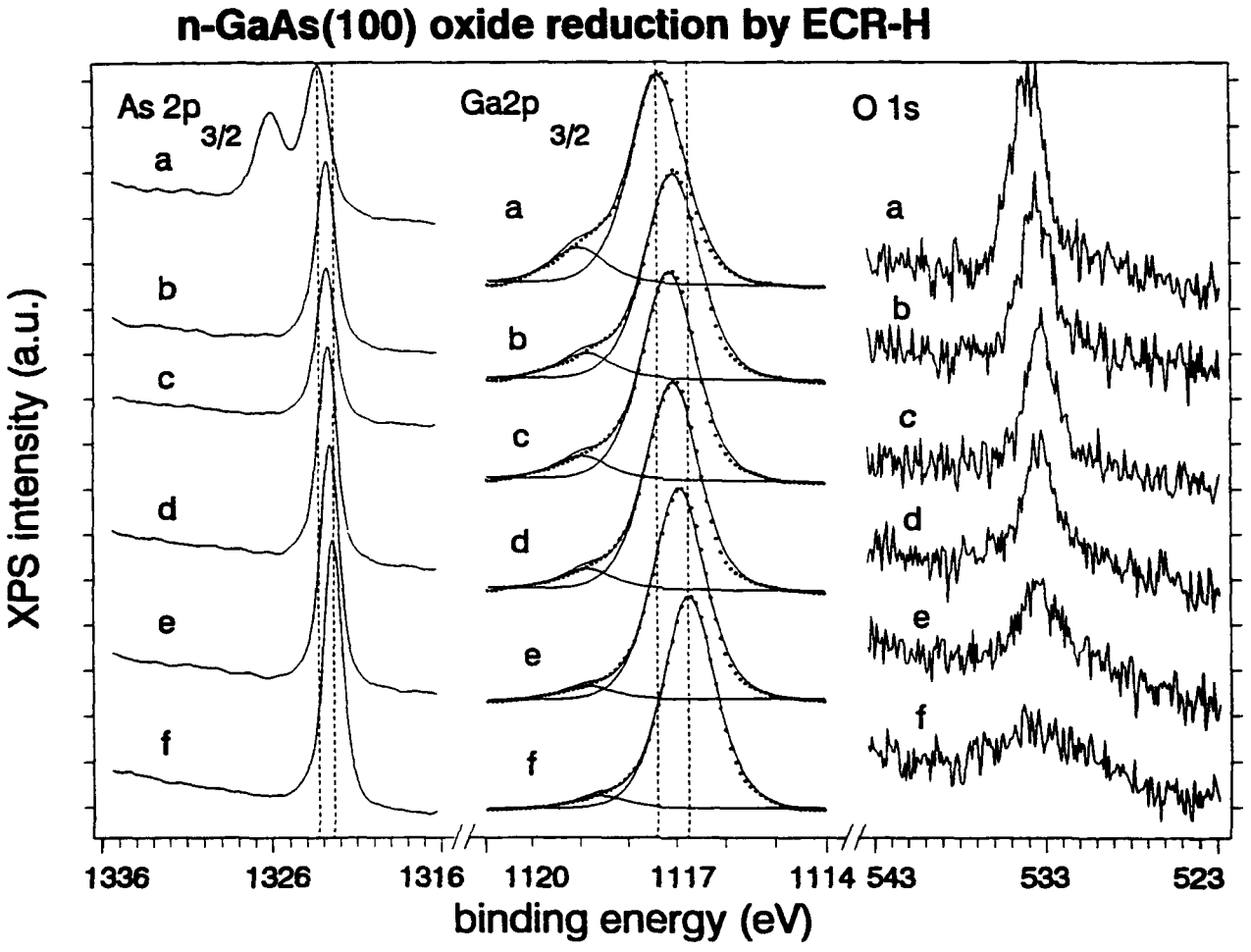

Figure 1. XPS spectra of the As $2p_{3/2}$, Ga $2p_{3/2}$ and O 1s core levels from n-GaAs (100): (a) for the initial surface prepared by H_2SO_4:H_2O_2:H_2O (10:1:1) solution after solvent cleaning; (b) after ECR hydrogen plasma processing for 10 min. at room temperature; (c) with an additional 20 min. exposure at room temperature; (d) after further processing for 20 min. at 170°C sample temperature; (e) after an additional 20 min. processing at 260°C and a final 20 min. processing at 350°C sample temperature; (f) spectra from a Ar^+ sputtered and annealed sample to show the characteristics of a completely clean surface.

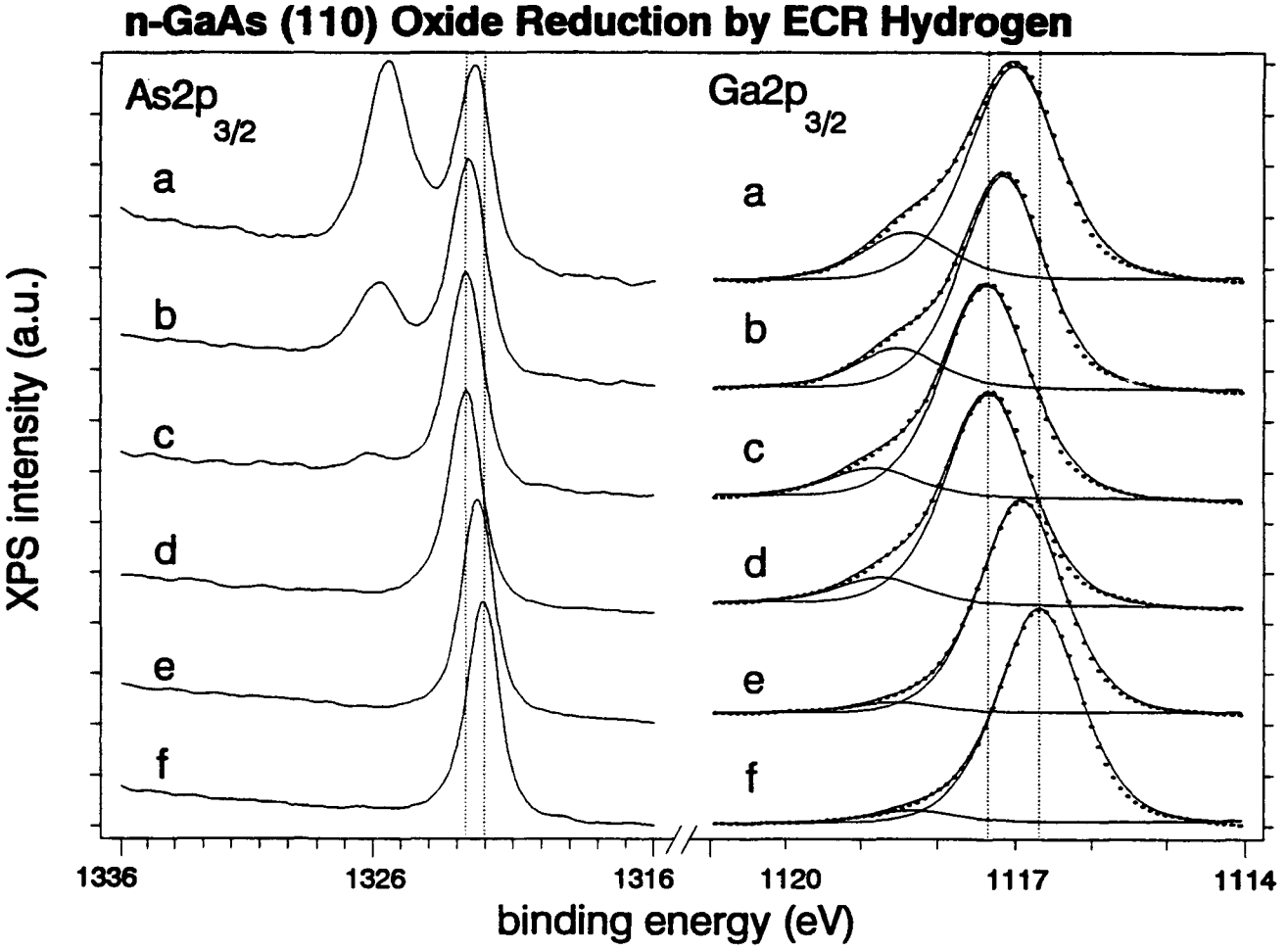

Figure 2. XPS spectra of the As $2p_{3/2}$ andGa $2p_{3/2}$ core levels from n-GaAs (110): (a) for the initial surface prepared by 50% NH_4OH (1 min.) after solvent cleaning; (b) after ECR hydrogen plasma processing for 20 min. at room temperature; (c) with an additional 20 min. exposure at room temperature; (d) after further processing for 15 min. at room temperature; (e) after an additional 20 min. processing at 300°C sample temperature; (f) final 20 min. processing at 300°C sample temperature.

ECR oxidation at room temperature forms a stoichiometric oxide layer which is primarily composed of As_2O_5 and Ga_2O_3 (see Fig. 3 and Fig. 4). A low energy electron diffraction study (LEED) observation showed that a hydrogen plasma can effectively clean GaAs surfaces and recover surface order, even at room temperature. Sample heating (200-300°C) expedited the removal of Ga_2O_3 and improved surface order.[3]

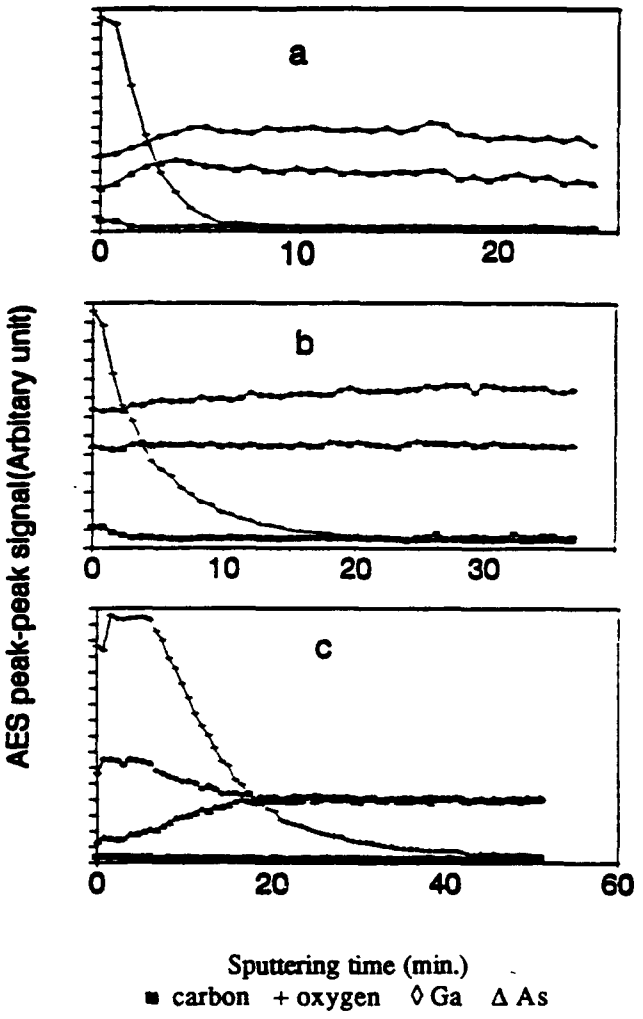

Figure 3. AES depth profile of ECR oxidized (110) n-GaAs surfaces. (a) ECR oxidation for 5 min. (oxide thickness is 22.1 Å); (b) oxidation plus post heating at 350°C for 10 min. to convert the chemical structure of the oxide; (c) oxidation plus post heating at 540°C for 15 min. which leaves the oxide Ga-rich.

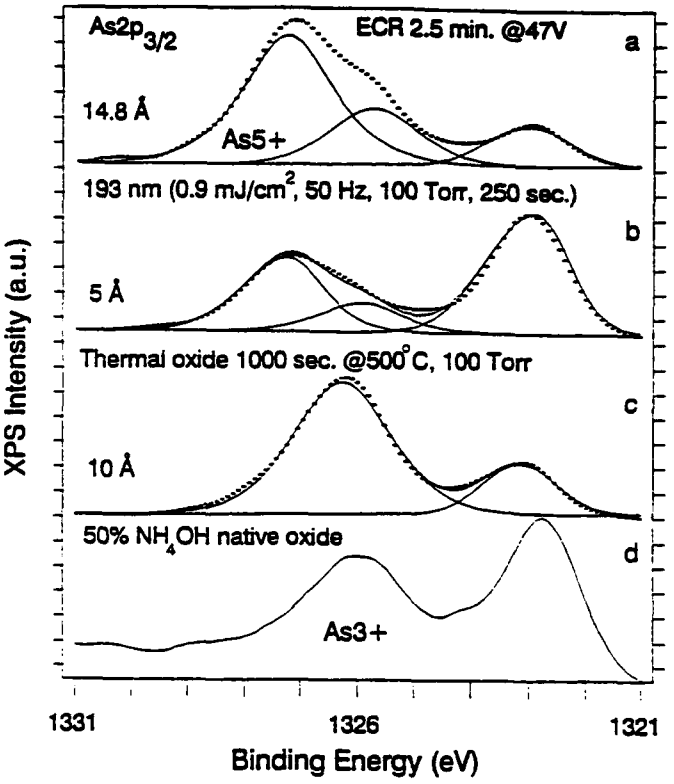

Figure 4. Oxidized GaAs surfaces formed under different oxidation conditions. (a) ECR oxidation; (b) 193-nm excimer laser grown oxide; (c) thermally grown oxide; (d) chemically cleaned surface.

We have also studied a thermal reaction of As_2O_5 with GaAs at temperatures below 500°C using MXPS.[4] A solid-state interface reaction of $4GaAs + 3As_2O_5 \rightarrow 2Ga_2O_3 + 3As_2O_3 + 4As$, which includes the usual native oxide thermal reaction of $2GaAs + As_2O_3 \rightarrow Ga_2O_3 + 4\,As$, as well as a decomposition reaction of $As_2O_5 \rightarrow AS_2O_3 + O_2$, is responsible for the thermal reaction in this temperature range as shown in Fig. 5.

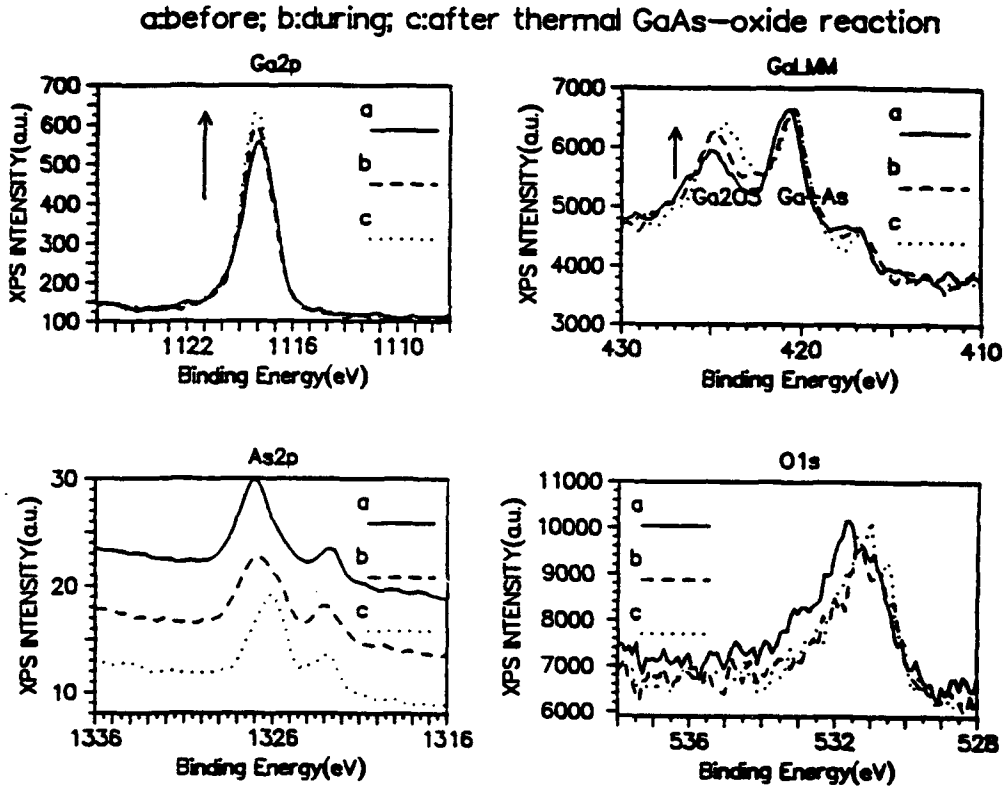

Figure 5. XPS spectra of As $2p_{3/2}$, Ga $2p_{3/2}$, O ls, and Ga LMM, for (a) AR^+ sputtering and annealed clean surface and then exposed to ECR oxygen for 30 sec.; (b) during the thermal conversion; (c) after the thermal conversion.

Similar ECR-H oxide removal studies have also been carried out on GaSb surface,[5] a material which has attracted a lot of interest recently for its applications in optoelectronic devices. Our experiments indicate that Sb-oxide removal occurs at room temperature while Ga-oxide removal occurs at a temperature of ~250°C, much lower than that for thermal evaporation of oxide (see Fig. 5). In addition, we have found that subsequent exposure of N_2 plasma leaves a thin nitride layer which prevents degradation of the H-cleaned surface and passivates the surface.

We have applied this technique to the processing of an AlGaSb PIN photodiode, which is fabricated of molecular-beam-epitaxy material. Our electrical measurement shows that the leakage current, after surface Sb-oxide removal, is significantly reduced from that before the ECR-H treatment (see Fig. 6).

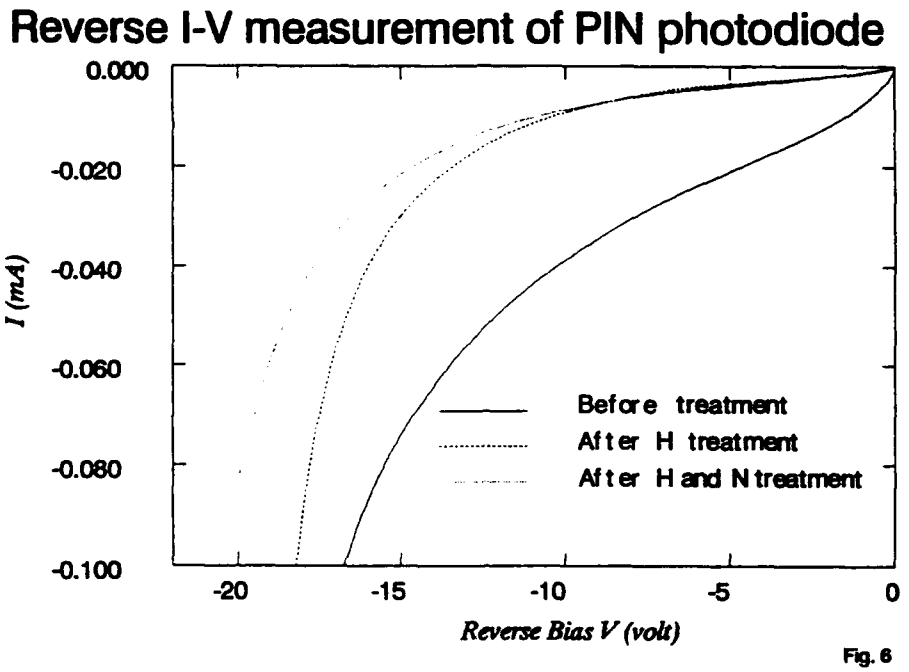

Figure 6. Reverse I-V curve of PIN photodetector.

Significant passivation effect has also been seen on AlGaAs/GaAs heterojuncion bipolar transistors by using ECR hydrogen and nitrogen plasma. As a result of the plasma processing, the base current ideality factor is improved from 2.67 to 1.96, and the maximum current gain is increased from 720 to 1000. In the low-current regime, the base current is reduced by two orders of magnitude.

Our work on oxide removal by ECR hydrogen plasma has large potential for molecular beam epitaxy applications. While MBE growth techniques have enjoyed great success for the fabrication of semiconductor materials with novel electrical properties, the regrowth of materials on previously processed wafers has not been extensively exploited. The main obstacle for GaAs regrowth is that standard growth preparation involves thermal cycling of a substrate to ~ 600° C to remove surface oxides and other contamination. Besides its inefficiency in removing carbon contamination, this thermal processing degrades the sharp interfaces grown by MBE, especially in the case of superlattice quantum layer materials, and pits the surface.

Our group has found that hydrogen plasmas can be used to effectively remove surface contamination (oxygen and carbon) from GaAs resulting in well ordered surfaces at much lower temperatures than those of standard techniques. The ability to remove, effectively and selectively, GaAs-oxide on a GaAs substrate by a hydrogen plasma will stimulate interest in its use for GaAs surface preparation and fabrication.

References:

1. Z. Lu, M. T. Schmidt, D. Chen, R. M. Osgood, W. Holber, D. V. Poldlesnik, J. Forster, Appl. Phys. Lett. **58**, 1143 (1991).

2. Q. Wang, E. S. Yang, P. Li, Z. Lu, R. M. Osgood, Jr., W. I. Wang, IEEE Electron Device Lett **13**, 83 (1992).

3. Z. Lu, M. T. Schmidt, R. M. Osgood, W. Holber, D. V. Podlesnik, J. Vac. Sci. Technol. A **9**, 1040 (1991).

4. Z. Lu, D. Chen, D. V. Podlesnik, R. M. Osgood, to be published, Proc. Mat. Res. Soc. Symp.: "Structure and Properties of Interfaces in Materials," Boston, Massachusetts, Dec. 2-7, 1991.

5. Z. Lu, Y. Jiang, W. I. Wang, M. C. Teich, R. M. Osgood, Jr., J. Vac. Sci. Technol.B **10**, (1992).

2. *In Situ* Optical Diagnostics of Semiconductors Prepared by Laser Chemical Processing and Other Novel Methods (I. Herman)

A model was developed that successfully describes etching of Cu films by Cl_2, as shown in Figure 1. It uses the calculated thermal distribution induced by the laser, and works best when the copper chloride film formed is thin.

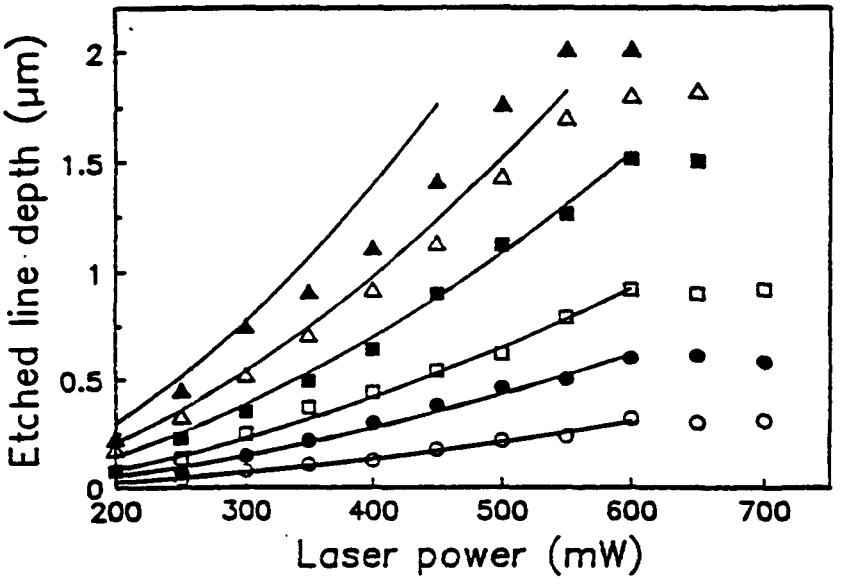

Figure 1. The etched copper depth (points for experimental data, lines for model simulation) on a passivated copper film (2.0 mm thick, 15 min. oxidation at 150°C) vs. incident laser power after the film was irradiated by a scanning laser beam (4880 Å, 200 mm/sec scan rate) for different chlorine pressures. The open circles, closed circles, open squares, closed squares, open triangles, and closed triangles represent data taken at 1, 2, 3, 5, 7, and 10 Torr Cl_2, respectively.

Polarization Raman scattering was used as an *in situ* probe of laser melting and etching in silicon. In particular, the peak height of the difference between the Raman spectra during laser melting and Cl_2-assisted etching of c-Si (Figure 2) is very similar to the etch depth (Figure 3) making Raman scattering a valuable real-time probe of etching.

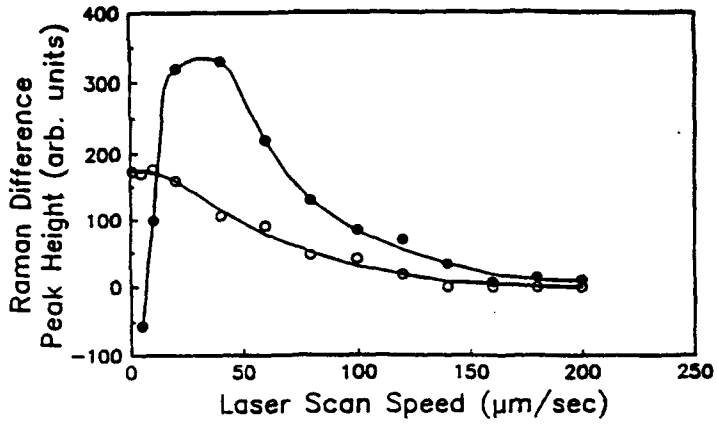

Figure 2. The peak height of the difference between the z(x,x)z Raman spectra during c-Si melting (100 Torr argon) and melting-assisted etching using either mixture A (open circles) and mixture B (solid circles) during scanning by a laser (1.6 W) in the x direction.

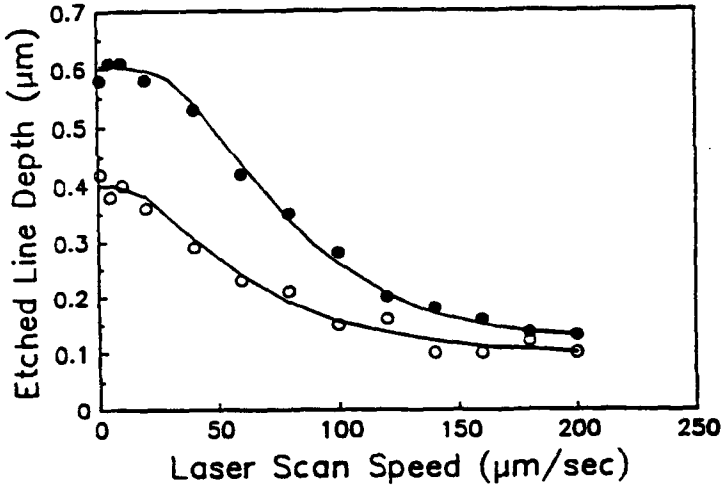

Figure 3. Profilometry measurement of the etched line depth vs. laser scan speed after c-Si melting-induced etching (1.6 W). The etchants are 0.3 Torr Cl_2/100 Torr Ar (mixture A, open circles) and 0.7 Torr Cl_2/100 Torr Ar (mixture B, solid circles).

Light emitting porous silicon films grown by H. Temkin and G. Higashi at AT&T Bell Laboratories were examined by Raman analysis. A typical spectrum is shown in Figure 4, which was fit to a model of phonon confinement in Figure 5. Spectra were independent of polarization, with data collected (Figure 6) and compared to the model. The localized structure is sphere-like rather than rod-like, with a lateral dimension of ~ 2.5 - 3.0 nm.

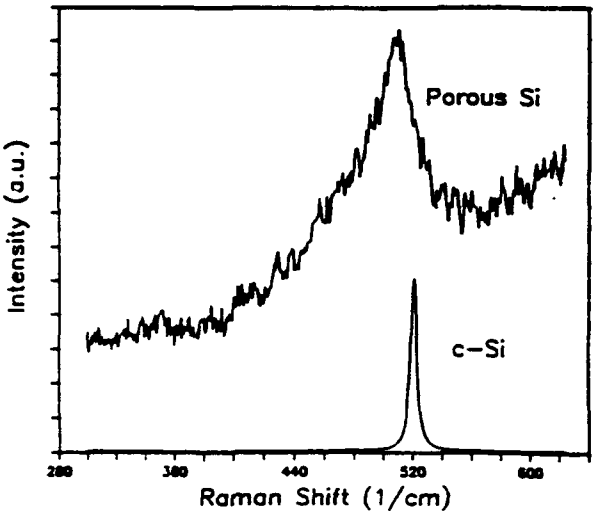

Figure 4. The unpolarized Raman spectrum of a thick light-emitting porous silicon film with the Raman spectrum of c-Si shown for comparison. The background in the porous silicon spectrum is due to the tail of the photoluminescence spectrum.

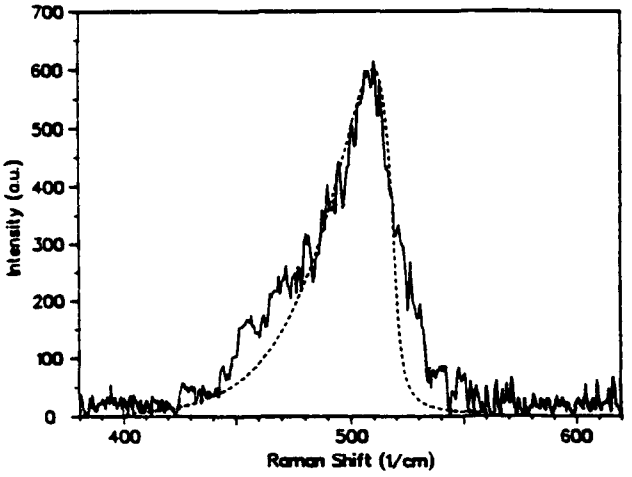

Figure 5. The background-subtracted Raman spectrum of porous silicon from Figure 4 compared with the spectrum calculated for a sphere with diameter L = 29 Å (dashed line).

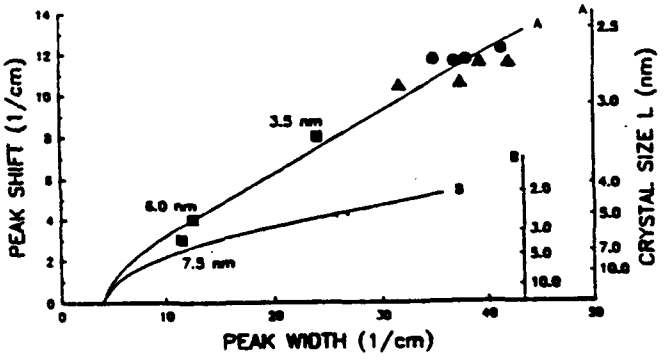

Figure 6. The calculated relationship between the Raman width, Raman shift relative to that of c-Si, and the nanocrystal size L for spherically-shaped nanocrystals (curve A, L is the sphere diameter) and cylindrically-shaped nanocrystals (curve B, L is the cylinder diameter). The triangles [circles] are the experimental data with perpendicular [parallel] incident and Raman polarizations, such as z(x,y)z [z(x,x)z] with respect to the unetched Si wafer, taken on different places on and along the edge of the film. The squares are published Raman data for μc-Si, with the crystallite dimensions listed from X-ray diffraction.

Studies of changing biaxial strains in semiconductor epilayers by applying hydrostatic pressure continued. A model was developed that shows that in strained layer heterostructures made of semiconductors from the same series, pressure always reduces strain, but can never make the structure free of strain (Figure 7). This strain free crossover can only occur in heterostructures made of semiconductors from different series, and then only when the phase transition pressure is suitably high (Figure 8). Use of the exact form of Murnhagan equations is necessary in these strain analyses (Figures 7 - 9).

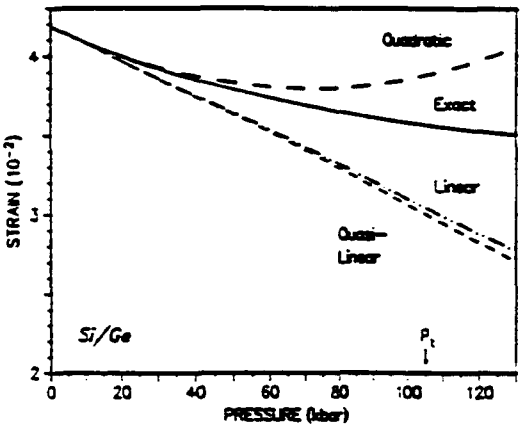

Figure 7. Linear, quasi-linear, quadratic and exact results for biaxial strain at room temperature are plotted versus applied hydrostatic pressure for a Si epilayer grown on a Ge substrate, which is a same-series semiconductor heterostructure. P_t denotes the lower of the two phase transistion pressures of the heterostructure component, i.e. for Ge.

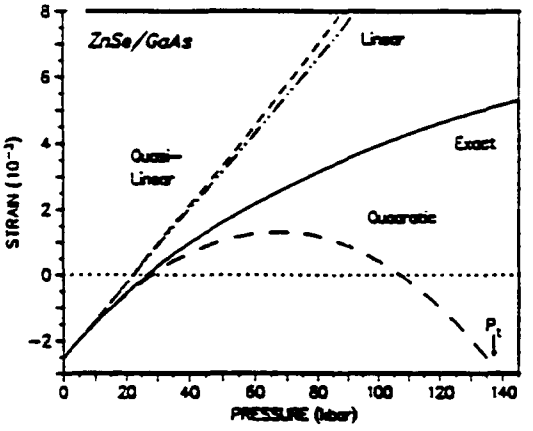

Figure 8. Linear, quasi-linear, quadratic and exact results for biaxial strain at room temperature are plotted versus applied hydrostatic pressure for a ZnSe epilayer grown on a GaAs substrate. In this different-series semiconductor heterostructure, each model predicts crossover through a strain-free condition at pressures lower than the phase transition pressure in each layer, which is in contrast to what happens in most other different series heterostructures. P_t denotes the lower of the two phase transition pressures of the heterostructure components, i.e. for ZnSe.

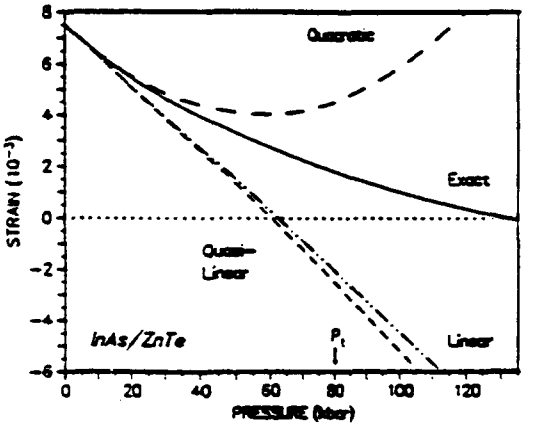

Figure 9. Linear, quasi-linear, quadratic and exact results for biaxial strain at room temperature are plotted versus applied hydrostatic pressure for an InAs epilayer grown on a ZnTe substrate. In this different series semiconductor heterostructure, exact theory predicts a crossover at a pressure far exceeding the transition pressure of each semiconductor, while the other models make incorrect predictions. P_t denotes the lower of the two phase transition pressures of the heterostructure components, i.e. for InAs.

3. Characterization of Semiconductor Surfaces and Interfaces with Femtosecond Optical Pulses (D. Auston)

Optical techniques have proven to be extremely valuable probes of the properties of semiconductors.[1] This report describes the basic concept and preliminary applications of the development of a new non-contacting technique for probing semiconductor surfaces and interfaces with femtosecond optical pulses. This approach measures the terahertz radiation produced when semiconductor surfaces and interfaces are illuminated with femtosecond optical pulses.[2] The mechanism is believed to be due to a rapid depolarization current arising from optically injected carriers in the electric fields associated with the interface. The amplitude and phase of the electromagnetic radiation from the semiconductor surfaces depend strongly on the material parameters and the specific structure of the interface region. We have systematically measured the dependence of the terahertz radiation on the carrier mobility, impurity doping concentration, and the strength and polarity of the static internal fields. A large selection of bulk, epitaxial layer and superlattice samples from III-V, II-VI and group IV semiconductors has been measured.[2-6] The amplitude and spectral distribution of the terahertz radiation arising from these samples has been characterized and correlated with built-in static fields due to surface depletion layers, metal/semiconductor Schottky barriers, p-n junctions, and strain-induced piezoelectric fields in strained-layer supperlattices.

When a semiconductor surface or interface is illuminated by an ultrafast laser pulse with the photon energy greater than the semiconductor bandgap, photons are absorbed, creating electron-hole pairs. If there is a static electric field at the surface or interface, the electron-hole pairs will form a dipole moment that is of opposite polarity to the field. If the injected carrier density is sufficiently low to avoid complete screening of the electric field, the depolarization current due to the rapidly increasing dipoles will radiate. Since the rise and fall times of this current can be very fast, the radiation will be in the terahertz region of the electromagnetic spectrum.

It has recently been suggested that the terahertz radiation could also be accounted for by a virtual depolarization current that does not require the generation of real charges.[7,8] This model has recently attracted a great deal of attention and appears to account for the terahertz radiation that we have seen when the optical wavelength is tuned just below the band gap where the absorption is negligible.[9] This effect has also been analyzed as an inverse Franz-Keldysh effect and has been given the name "virtual photoconductivity". When the photon energy is above the band-gap, it has been suggested that the virtual depolarization effect can also give rise to a signal that will compete with the signal due to real drift currents.[7] The specific conditions for which the real and virtual currents are expected to dominate is not yet fully understood. However, we might expect that the virtual current would be more likely to dominate on shorter time scales since the real current is not well defined until the carriers have experienced a number of collisions, which can require a few hundred femtoseconds. Also, at very high fields, the real drift current will saturate due to phonon emission, and is expected to make a smaller relative contribution.

As illustrated in Fig. 1, the radiation from the semiconductor surface has inward (transmitted direction) and outward (pseudoreflected direction) components. The tilted wavefront of the optical beam determines the timing of the photocurrent distribution. If the optically illuminated area is comparable to or larger than the radiation wavelength (typically 0.5 mm), the electromagnetic pulse is directional and diffraction-limited.[10] The incident optical angle θ_{op}, propagating direction of outward radiated field θ_1 and inward radiated field θ_2 satisfy a generalized Fresnel law:

$$n_1(\omega_{op})\sin\theta_{op} = n_1(\omega_{el})\sin\theta_1 = n_2(\omega_{el})\sin\theta_2$$

where $n_2(\omega_{el})$ is the index of refraction of radiated field of the sample, $n_1(\omega_{op})$ and $n_1(\omega_{el})$ are the indices of refraction of the optical beam and the radiated field outside of the sample, respectively. Since the difference between $n_1(\omega_{op})$ and $n_1(\omega_{el})$ is negligible in the air, the direction of the

pseudoreflected (backward) electromagnetic radiation is near the specular angle of the laser beam, resulting in $\theta_{op} \approx \theta_1$.

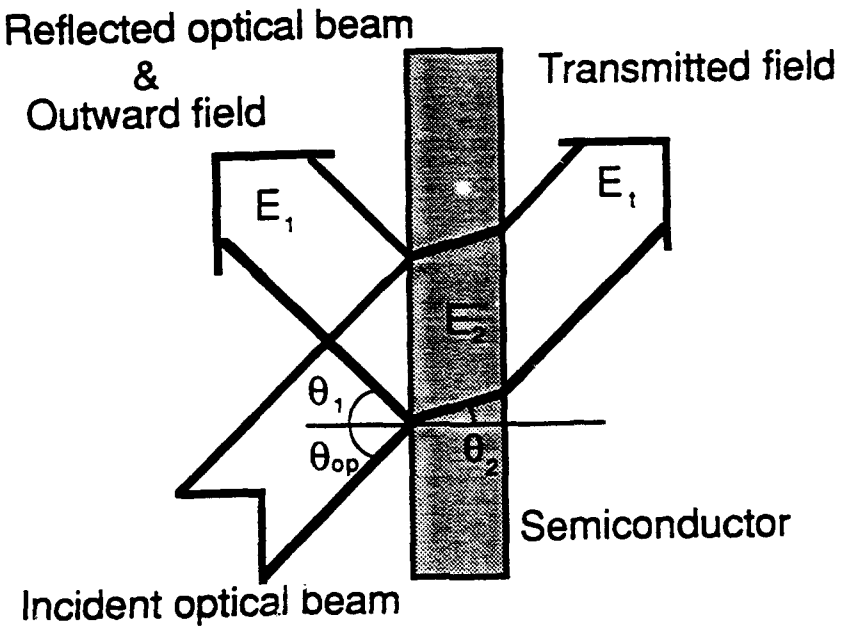

Figure 1. Electromagnetic beams generated from semiconductor surface. The incident optical beam, the outward radiated field and inward radiated field satisfy the generalized Fresel law.

The amplitude of the radiated field strongly depends on the optical incident angle. For example, the angular dependent radiated field as a function of the incident angle has the following form:

$$E(\theta) \propto \sin(\theta)\,[1-R(\theta)]\,t(\theta)$$

The first term comes from the radiation pattern of the dipole approximation, the second term from the photocarrier density which is proportional to the optical absorption, and the third term from the transmission coefficient of the electromagnetic wave. This equation can be further expanded as:

$$E(\theta) \propto \sin(\theta)\left[1-\left[\frac{\tan(\theta-\theta_2)}{\tan(\theta+\theta_2)}\right]^2\right] \frac{2\cos(\theta)\sin(\theta_2)}{\sin(\theta+\theta_2)\cos(\theta-\theta_2)}$$

where $\theta_2 = \sin^{-1}(\sin(\theta)/n_2)$ with n_2 the index of refraction of the radiated field. The maximum radiation direction is close to the Brewster angle, and its amplitude is proportional to the optical power, the carrier mobility, and the integral of the product of the built-in field and the photocarriers.

For a moderate incident optical power density, a reduction in the magnitude of the static field by the space charge screening from the photocarriers can be ignored. In this case the static field is independent of time and does not change even with the optical excitation. As a result, the amplitude and polarity of the radiated electromagnetic field in weak incident optical power is proportional to the strength and sign of the static built-in field.

The radiation field is proportional to the number of the photocarriers, but this is only valid under the assumption of low optical excitation. When the incident optical power reaches a level at which the photocarrier density is comparable to the background doping density of the semiconductor, the emitted radiation will saturate. We can estimate an upper bound on the radiated energy from the energy E_s stored in the static electric field:

$$E_s = \frac{1}{2}\kappa E^2 d$$

where d is the field length. For a GaAs sample with 1 V across d = 0.1 μm, Es is approximately 50 nJ/cm^2. If all the energy can be released within 1 ps, the upper bound on the radiated energy from one square centimeter area is 50 kW peak power.

The coherent detection of the terahertz pulses uses a photoconducting dipole antenna, fitted with a 3.2 mm truncated sapphire ball to enhance the collection efficiency.[11-13] We had previously developed this technology for detection of terahertz radiation from photoconducting antennas with external bias fields.[10] The spectral range of our detector extended to approximately 1 terahertz.

Many varieties of samples of III-V, II-VI and group IV semiconductors have been measured. For the semiconductors with bandgaps much larger than the laser photon energy ($\hbar\omega$ = 2 eV), no radiation process is expected, and this has been verified by ZnSe (Eg = 2.4 eV) and GaP (E_g = 2.2eV). We have achieved electromagnetic radiation from InP, GaAs, $Ga_{1-x}Al_xAs$($x<0.2$), GaSb, InSb, CdTe, CdSe, Ge and Si; all these samples have bandgaps less than the incident photon energy. The amplitudes of the radiated fields of different samples are listed in Table I, where the amplitudes are normalized to that of the InP sample. Si and GaSe show moderate signals, because the absorption lengths in Si and GaSe at an optical wavelength of 620 nm are approximately 10 times longer than those in InP and GaAs, causing few carriers in the depletion layer to contribute to the radiation. Among these samples, the radiation strength of semi-insulating InP is 200 times stronger than that of Si. The <100>-oriented semi-insulating iron-compensated InP, which shows the strongest optical induced electromagnetic radiation, has been analyzed by Auger spectroscopy and found to have a 15 angstrom oxide layer on the surface. Different semiconductors show different radiated waveforms.

Table I

Sample	InP	GaAs	CdTe	CdSe	InSb	Ge	GaSb	Si	GaSe
Signal	100	71	33	11	8	7	2	0.5	<0.1

Table I. The amplitude of the outward radiated field of several semiconductor samples at room temperature.

Figure 2(a) shows a typical waveform of the radiated field from semi-insulating InP, detected by the dipole antenna in the outward direction (45 degrees relative to the normal) with a 4 mm nominal diameter laser beam. Figure 2(b) is the frequency spectrum of the temporal waveform. A 16.2 degree diffraction angle of the radiated power has been measured at far field. This value agrees well with the diffraction theory value of 15 degrees. The amplitude of the radiation field is found to be linearly proportional to the low optical pulse energy from 2 to 100 pJ.

Due to the resonance behavior of the dipole detector and slow response of the photoconductor, the bandwidth of the radiation is limited by the detection bandwidth. A recent study of the bandwidth of the radiation by using interferometric technique found a 160 femtosecond electromagnetic pulse duration from InP sample with an amplified laser beam.[14] The frequency component ranged from 3 to 150 cm^{-1}.

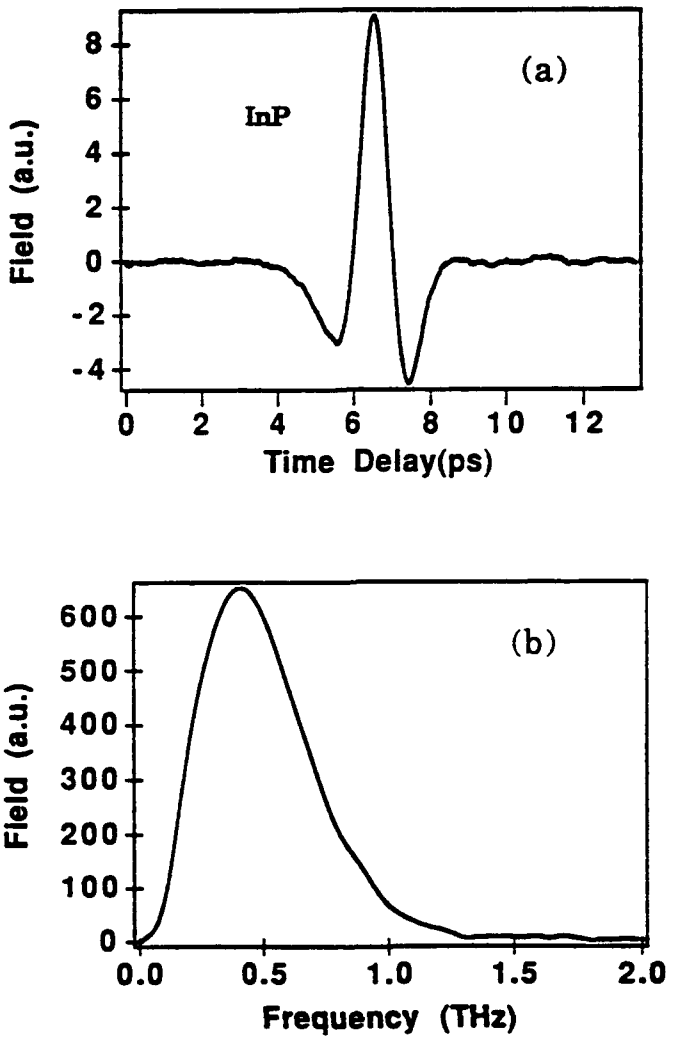

Figure 2. (a) Waveform of the outward electromagnetic radiation from a semi-insulating InP with $\theta_{op} = 45$ degrees; (b) frequency spectrum of the temporal waveform.

We have measured the angular dependent radiation by measuring the transmitted electromagnetic wave through a 0.4 μm thick semi-insulating InP wafer as a function of the incident angle. In this measurement, a 0.5x5 cm InP wafer was placed in the laser beam path before the dipole detector and the wafer was rotated horizontally around its symmetry axis parallel to the 0.5 cm edge. The result of the radiation field vs the rotation angle measurement is plotted in Figure 3. The solid dots are experimental data and the curve is a calculation. The agreement between the experimental result and calculated curve confirms so that the flow direction of the photocurrent is normal to the surface. The amplitude ratio of the TM wave (polarization in the incident plane) to TE wave (polarization normal to the incident plane) is over 20:1.

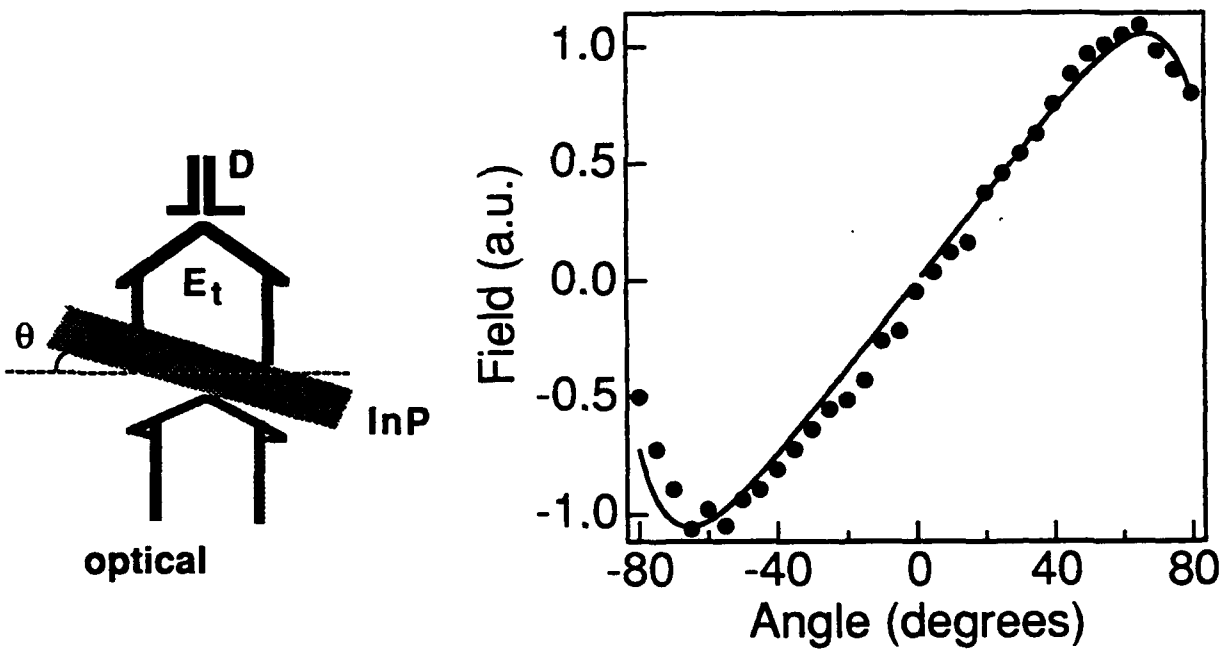

Figure 3. (a) Angular dependent experimental setup. D is a 100-μm dipole antenna detector; (b) transmitted amplitude of radiated field E_t as a function of the rotated angle of InP with measured data (dots) and theoretical calculation (curve).

Since the direction of the surface depletion fields are opposite in n-type and p-type samples, the radiated waveforms from these samples should have opposite polarities. Figure 4 shows the radiated field from n-type ($n \approx 10^{18}/cm^3$) and p-type ($p \approx 10^{18}/cm^3$) GaSb samples. The opposite polarity of the radiated fields from n-type and p-type samples indicates opposite static surface fields. The amplitude of the n-type sample is larger than that of the p-type sample. This is believed to be due to the different values of the surface fields. Similar results were also achieved from GaAs samples ($n,p \approx 10^{16}/cm^3$). We observed slight waveform shape changes between n-type and p-type samples. The radiation pulses from the p-type samples have richer high-frequency components than those from the n-type samples. This difference also comes from the different values of the surface built-in potential, resulting in different depletion widths and different radiation waveforms. For p-type GaAs and GaSb samples, the surface fields are smaller and the depletion widths are short compared with those of n-type samples; therefore, the amplitude of the radiated fields from the p-type samples are weaker and the pulses are faster.

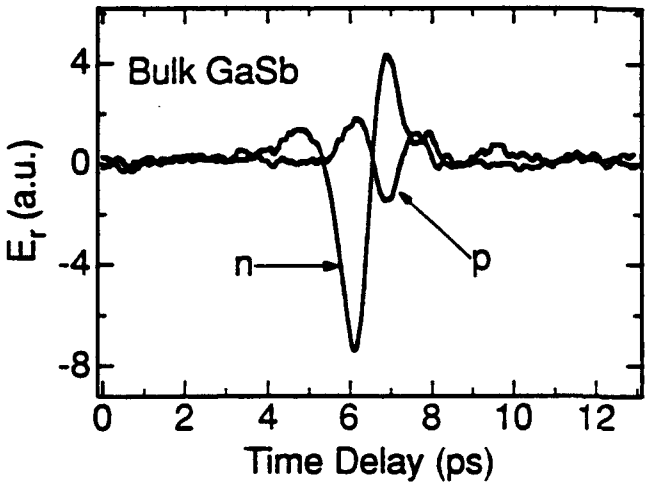

Figure 4. Radiated waveforms of both n-type and p-type bulk GaSb. Opposite polarity of the waveform reflects the opposite direction of the depletion field of the different type doped GaSb samples.

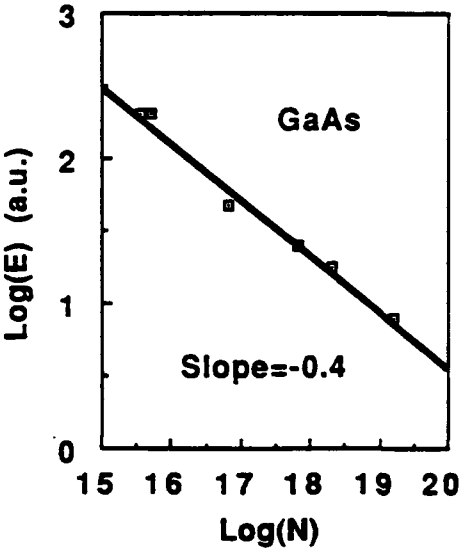

Figure 5. The amplitude of the outward radiated field E vs the doping concentration N from GaAs samples plotted on a logarithmic scale. A slope of - 0.4 is measured.

We have investigated the strength and polarity of the surface fields by using several n-type and p-type GaAs samples with doping concentrations from 10^{15} /cm^3 to 10^{19} /cm^3 and semi-insulating LEC GaAs samples. The results are listed in Table II. A higher doping concentration reduces the radiation field due to the absorption of submillimeter waves from the conducting substrate. The absorption coefficient at submillimeter wavelengths is proportional to the square root of the doping level. There are other effects of doping which have not been well characterized, such as the dependence of the transient carrier mobility on the doping level. In Table II, the n-type samples show the opposite polarity compared with the p-type samples. As we mentioned before, this difference is a result of the opposite directions of their depletion fields due to the different type of majority carrier. For the undoped GaAs (LEC), the energy level of EL2 makes it close to n-type, therefore the waveform of the radiated field of undoped GaAs has the same polarity as that of n-type GaAs. Figure 5 shows the amplitude of the outward radiation from doped GaAs for a range of impurity concentrations N, from 10^{15} /cm^3 to 10^{19} /cm^3 on a logarithmic scale. A simple analysis developed in the following section predicts that the amplitude of E_{out} is proportional to the inverse of the square root of the doping concentration N, $E \propto N^{-0.5}$. We have observed $E \propto N^{-0.4}$ in the GaAs samples. The difference in the exponent (- 0.5 vs - 0.4) comes from the absorption and reflection of the submillimeter wave by the substrate.

Table II

N (cm^{-3})	LEC	3.5×10^{15}	6.7×10^{16}	6.3×10^{17}	2.0×10^{18}	1.6×10^{19}
μ (cm^2/V.sec)		4958	263	2975	1997	47.4
ρ (Ohm.cm)		36.1	35.4	0.33	0.153	0.85
doping	n	n	p	n	n	p
Amplitude(au)	+ 1.7	+ 2.02	- 0.47	+ 0.25	+ 0.18	- 0.08

Table II. The amplitude of the outward radiated field from GaAs samples with different doping concentrations. The polarities of the radiated fields from n-type samples and p-type samples are opposite. Mobilities and resistivities are listed also.

The sign and approximate magnitude of the surface fields at metal/semiconductor Schottky barriers has also been estimated by our measurements. This is illustrated in Figure 6. Thin gold films were evaporated on n-type and p-type GaAs (111) wafers (n, p ≈ 10^{16}/cm^3). The thickness of the gold films were varied from 40 to 80 angstroms, which allows greater than 60% laser beam transmission. The wafers were chemically cleaned and heated in ultrahigh vacuum to 550°C to produce clean surfaces prior to gold deposition in the same vacuum system. An indium contact on the back of the sample was annealed to provide an ohmic contact. The Schottky samples show good rectifying behavior in current-voltage measurements. Therefore, a bias on the Au film results in a uniform modulation of the electric field at the semiconductor surface.

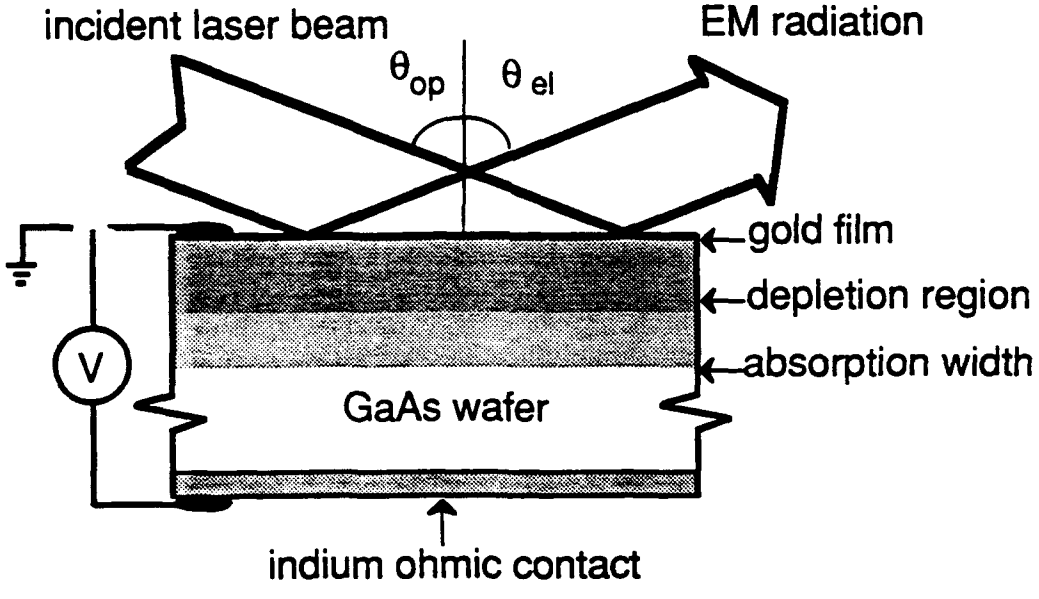

Figure 6. Schematic illustration of the outward radiated field from an Au/GaAs Schottky Barrier with an external bias (the inward radiation is not shown). For GaAs samples with a doping level greater than 10^{16} /cm^3, the depletion width is less than the photon absorption width.

For a moderate bias voltage the external potential is mainly applied across the Schottky barrier and changes the depletion width W. For high forward bias, the high current causes the bulk resistance to reduce the potential affecting the Schottky barrier, and the built-in field can not be completely eliminated. For high reverse bias, the field across the depletion region causes

breakdown of the Schottky diode, again limiting the effect of the surface field. The externally controlled surface field can be monitored by the radiated terahertz signal.

We can find a simple relation between the radiation field and the surface depletion width W. If the depletion width W is much less than the optical absorption length α^{-1} ($W<<\alpha^{-1}$), which is generally true for carrier concentrations $N>10^{16}$ /cm^3, the photocarrier density is nearly uniform within the depletion width. Furthermore, Monte Carlo calculations show that the drift velocity saturates with the electric field for fields greater than 5 kV/cm.[15] The calculations are based on a colliding pulse mode-locked (CPM) laser pulse excitation (100 fs pulse duration and 2 eV photon energy), and the temporal range of the calculated velocity is over one ps. Therefore the drift velocity v is saturated by the field in the depletion region (not sensitive to the position x) and can be assumed to be a constant. With the above approximations, the amplitude of the radiated field E_r is simply proportional to the depletion width W:

$$E_r \propto W$$

where W depends on the impurity level N and surface potential V.

Figure 7 shows the amplitude (squared) of the radiated signal from n-type GaAs with a 40 angstrom Au film vs applied bias voltage. The radiated field increases at a moderate reverse bias on the n-type sample and saturates at higher reverse bias. Basically, the reverse bias enhances the internal (built-in) field and increases the depletion width, while the forward bias cancels the internal field. The direction of reverse bias (as well as forward bias) of n-type and p-type Schottky barriers is opposite. Since $E^2 \propto W^2 \propto (V + V_{bias} - kT/e)$, the static built-in potential V can be estimated from the intersection point where $V_{bias} = kT/e - V$ in Figure 7. We have estimated that the built-in field V has a value of 0.81 ± 0.05 eV for n-type Au/GaAs Schottky sample. In principle, the analysis of experimental data is analogous to electronic C-V measurements.

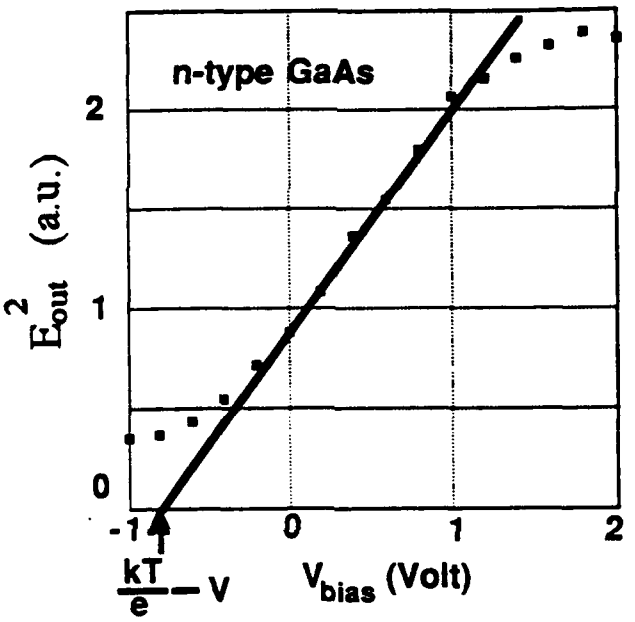

Figure 7. The amplitude square of the outward radiated field vs an external bias voltage on the Schottky barrier from n-type (positive bias voltage → reverse bias), where $V_{bias} = kT/e - V$ at the intersection point.

Similar to the analysis of the n-type Au/GaAs Schottky barrier, we have estimated $V = 0.32 \pm 0.1$ eV for p-type Au/GaAs Schottky barrier. The radiated field of n-type GaAs at zero bias is about 5 times stronger than that of p-type. Also the increased experimental error in the p-type sample is from the larger leakage current in our p-type Schottky diode.

The misfit strain in a lattice misfit superlattice, in general, can be accommodated by the elastic deformation and misfit dislocation formation. For a sufficiently thin layer in the superlattice, the tetragonal distortion is the dominant process to accommodate the strain. The macroscopic polarization P_i induced by the strain is proportional to the off-diagonal components of the strain tensor, ε_{jk}. The strain induced polarization has a form of $P_i = 2e_{41}\varepsilon_{jk}$, with the piezoelectric coefficient e_{41}. Since $e_{jj} = 0$, the diagonal strains do not induce a polarization for <100>-growth-axis strained-layer superlattice. Any other growth direction strained-layer superlattices show the strain induced polarization.[16] Particularly in a <111> oriented strained-layer superlattice, the strain-induced macroscopic polarization generates an electric field along the <111> growth axis.[17] The amplitude of this piezoelectric field is given by:

$$E_{<111>} = \frac{2e_{41}}{\sqrt{3}k}(\varepsilon_{xy} + \varepsilon_{yz} + \varepsilon_{xz})$$

The sign of the off-diagonal symmetric strain tensor ε_{jk} depends on the biaxial compression and expansion (tetragonal distortion) of the layers. The direction of the piezoelectric field in the layer depends on the type of distortion of the layer (contraction or expansion) and the grown face of the substrate. For the layer which has a small lattice constant and suffers expansion, the piezoelectric field from an A-face (B-face) superlattice points inward (outward).

The ratio of the piezoelectric fields of the well $|\vec{E}_w|$ and the barrier $|\vec{E}_b|$ depends on the lattice constant of the thick buffer layer grown on the substrate. The layers (barriers or wells) with a lattice constant close to the lattice constant of the buffer layer have a smaller strength piezoelectric field, since the layers have less distortion and strain. The strength of the piezoelectric fields in some strained-layer superlattices can be as high as 10^5 V/cm.

The piezoelectric field provides a suitable bias for generating optically induced electromagnetic radiation. The radiated fields from the strained-layer superlattices, such as GaSb/AlSb, InGaSb/InAs and InGaAs/GaAlAs, have been measured and analyzed. The structures of InGaAs/GaAlAs, GaSb/AlSb and InGaSb/InAs samples are listed in Table III to Table VI, respectively. All the multiquantum wells and superlattices were designed to have thick buffer layers. For the lattice constant of the buffer layer equal to the average lattice constant of the superlattice, the piezoelectric field alternates in the constitute layers. For the buffer which is lattice matched to the quantum wells (or barriers), the quantum wells (or barriers) have essentially no distortion, leading to no strain and no piezoelectric field. The orientation of the piezoelectric field in the layer depends on the distortion type of the layer (contraction or expansion) and the growth face of the substrate. For the well which has a small lattice constant and suffers expansion, the inward or outward direction of the field depends on whether the superlattice is grown on the A-face or B-face substrate. The piezoelectric in <111> oriented strained-layer superlattices have been confirmed by optical and optoelectronic techniques.[17-20]

Table III

Sample	GaAs	InP	Ge	GaSb	InSb
E(T=300K)	4.1	9.8	0.7	0.5	0.8
α	1.7	3.4	3.7	4.0	4.1
β	3.4	7.1	11	18	21

Table III. The ratios of the radiated peak value (α=E(T=80K)/E(T=280K)) and radiated energy value (β=W(T=80K)/W(T=280K)) from several semiconductors. For comparison, the relative strengths of the radiated field at 300 K are shown also.

Table IV

sample #	L_b (AlSb) Å	L_w (GaSb)Å	periods (N)
545a,b	300	400	10
544a,b	300	300	15
595a,b	150	150	20
596a,b	150	100	20

Table IV. The parameters of 4 pairs of <100> and <111> B oriented GaSb/AlSb superlattices. Sample #544a is the <100> oriented superlattice, #544b is the <111> oriented superlattice, and so forth in the other pairs. The top layers are GaSb.

Table V

sample #	L_b (InGaAs)	L_w (AlGaAs)	periods (N)
426a,b	300	400	10
427a,b	300	300	15
428a,b	150	150	20

Table V. The parameters of 3 pairs of <100> and <111> B-face InGaAs/AlGaAs superlattices. The top layers are GaAs.

Table VI

sample #	L_b ($In_{0.4}Ga_{0.6}Sb$) Å	L_w (InAs) Å	periods (N)
740a,b,c	40	40	50

Table VI. Samples #740 a, b and c are the InGaSb/InAs superlattices having <100>, <311>B and <311>A orientations. They are type II, staggered superlattices. The top layers are $In_{0.4}Ga_{0.6}Sb$.

Four pairs of GaSb/AlSb strained-layer superlattices and one pair of GaSb thin film samples grown on <100> and <111>B (4 degrees off from the <111> direction) oriented GaAs wafers by molecular beam epitaxy (MBE) were used in this experiment. The sample structures are shown in Figure 8. In the GaSb/AlSb quantum well structure, GaSb (E_g = 0.69 eV) forms the quantum wells, while AlSb (E_g = 1.6 eV) forms the barriers. The width of the quantum wells varies from 100 Å to 400 Å for different superlattices. The GaSb films have a thickness of 5000 Å. The conduction band and valence band offsets in the superlattices are approximately 0.5 and 0.4 eV, respectively, giving strong spatial confinement for both electrons and holes. The superlattice and film samples are not intentionally doped; Hall measurements show that all samples are p-type and have a typical impurity level of 8.2 x 10^{15}/cm^3.

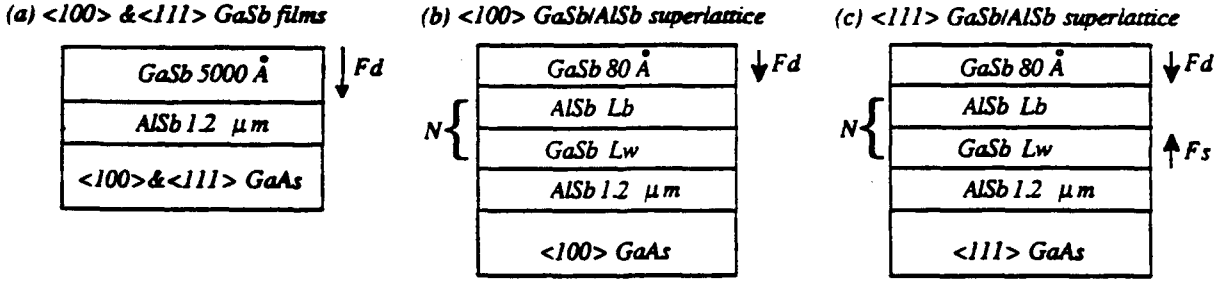

Figure 8. The schematic structures of GaSb/AlSb superlattice and GaSb thin-film samples. F_d and F_s are the surface depletion field and the strain-induced field, respectively. The directions of the fields are labeled as the directions of the arrows.

The Fermi level in these p-type samples "pins" the energy bands downward near the surface and forms the depletion field having a direction inward to the substrates. The samples should show the same p-type behavior in the electromagnetic waveforms if the only contribution to the radiation is from the surface depletion layer. A larger radiation amplitude from the GaSb films than that from the superlattice GaSb cap layer (80 Å thick) is expected due to the greater number of photocarriers in this region. When the strain-induced electric field contributes to the electromagnetic radiation, the waveforms from the <111> oriented GaSb/AlSb superlattices should be very different from the others. For a free-standing <111> oriented strained-layer superlattice, piezoelectric fields exist both in the wells and the barriers, and their directions are opposite. With a thick (1.2 μm) AlSb as a buffer layer for the superlattice, the lattice distortion in the AlSb barriers is much less than in the GaSb wells, and the strain in the AlSb barriers is negligible compared with that in the GaSb wells. Furthermore, in <111> oriented GaSb/AlSb superlattices with the optical excitation energy of 2 eV, the radiation from the quantum barriers is much weaker than that from the quantum wells because of the moderate field strength and smaller absorption coefficient (indirect band minimum for AlSb, direct band minimum for GaSb) in the barriers. Since the <111> oriented superlattices were grown on <111> B-face substrates, the direction of the strain-induced field in the GaSb quantum wells, which have a smaller lattice constant and suffer compression, points outward, opposite to the surface depletion field for p-type samples. The strain-induced field overrides the surface and barrier fields, resulting in an outward macroscopic electric field.

The samples were mounted in a cryostat at a temperature of about 80 K, with their front surfaces aligned to the same plane to equalize the timing for the temporal waveform measurement. The incident angle of the laser beam was 55 degrees and the optical power density on the sample was 3 mW/cm^2. The radiated electromagnetic pulses at the specular angle were collected by two gold-coated off-axis parabolic mirrors and were focused on a photoconducting antenna by an attached sapphire lens. Figure 9 shows the radiation waveforms from two GaSb films and a pair of superlattices (samples #544a,b) at 80 K. The waveforms (p-type samples) from the surface

depletion fields of the two GaSb films and the <100> superlattice are similar, while the waveform from the <111> superlattice is like that of an n-type sample, opposite from the others, as we expect from the opposite direction of the strain-induced field. The radiation from the piezoelectric field in the <111> superlattice clearly overrides the contribution from the surface depletion field. The amplitude (absolute value) from the <111> superlattice is 8.6 times larger than that from the <100> superlattice. The other three pairs of GaSb/AlSb superlattice samples show similar behavior. The waveforms radiated from the <111> superlattices are opposite to those from the <100> superlattices.

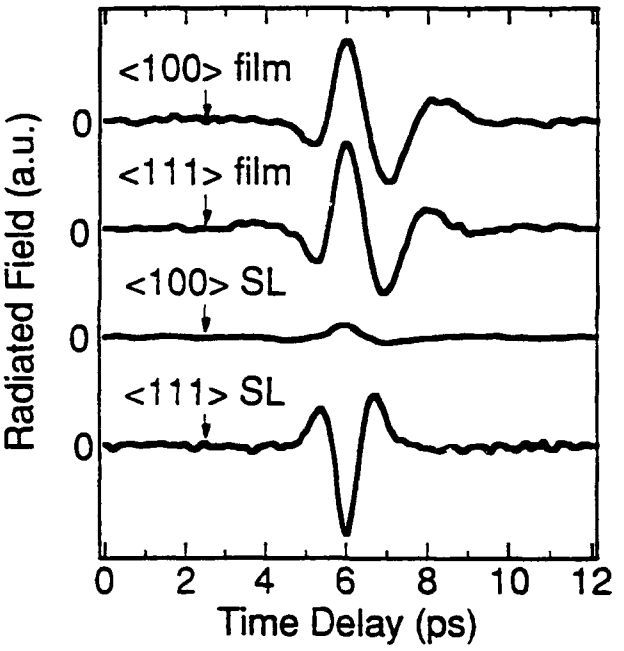

Figure 9. Waveforms of optically induced electromagnetic radiation from <100> and <111> oriented GaSb films and GaSb/AlSb superlattice samples #544a,b. The waveform from the <111> superlattice is opposite to the others due to the piezoelectric field in strained quantum wells opposite to the surface depletion fields in the p-type GaSb cap layers.

A pulse duration of 450 fs (full width at half maximum) is measured for the <111> superlattice and 800 fs for the films (without deconvolution). The time domain waveforms were transformed to the frequency domain for a better comparison. Figure 10 shows the frequency spectrum of the <111> film and the <111> superlattice. The spectrum of the film peaks at 0.4

THz while the spectrum of the <111> superlattice is completely limited by the detector response, which has been calibrated by electro-optic Cherenkov radiation from a $LiTaO_3$ crystal.[13] We also observed that the spectra from the <111> superlattices with narrower well widths are richer in high frequency components than the spectra from wider wells, but have lower amplitudes due to the poor antenna efficiency at the higher frequencies.

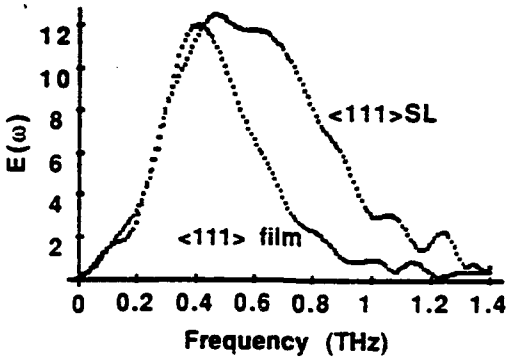

Figure 10. Fourier spectra of the temporal waveforms: (a) <111> oriented GaSb film; (b) <111> oriented GaSb/AlSb superlattice sample #544b.

We also measured the radiation from strained-layer InGaAs/GaAlAs superlattices. The experimental setup is identical to that for GaSb/AlSb. The structures of <100> and <111>-oriented $In_{0.2}Ga_{0.8}As/Ga_{0.6}Al_{0.4}As$ samples (#428a, b) is shown in Figure 11. The radiated signals from the samples are (#428a, b) plotted in Figure 12. Once again, similar to the data from the GaSb/AlSb sample, the radiation from the <100>-oriented InGaAs/GaAlAs sample is weaker than that from the <111> sample, and opposite polarity of the waveforms is observed.

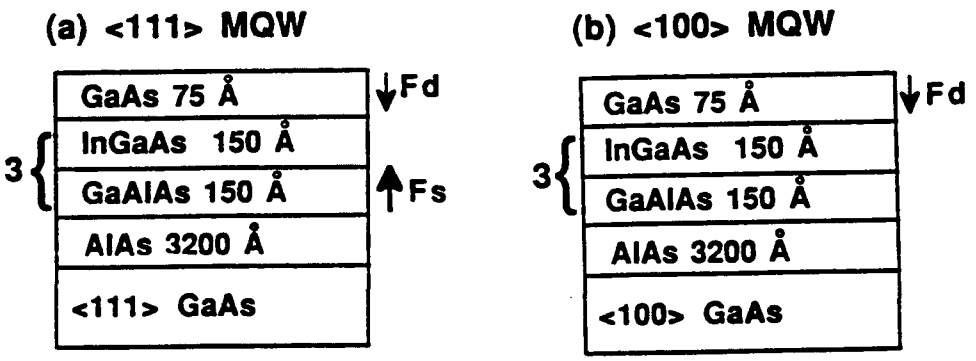

Figure 11. The schematic structures of strained-layer InGaAl/GaAlAs superlattices.

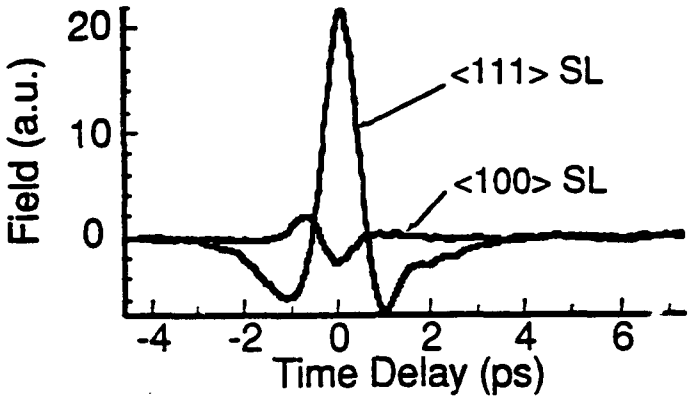

Figure 12. Waveforms of the radiated field from the <100> and <111> oriented InGaAl/GaAlAs superlattices.

Three $Ga_{0.6}In_{0.4}Sb$/InAs samples (with <100>, <311>A and <311>B orientations) grown by molecular beam epitaxy (MBE) were used in our experiment. The samples grown on GaAs substrates have a 1-μm AlSb buffer layer followed by 50 periods $Ga_{0.6}In_{0.4}Sb$/InAs superlattice, as shown in Figure 13. The thickness of each layer is 40 Å. The cap layer is 40 Å $Ga_{0.6}In_{0.4}Sb$. The $Ga_{0.6}In_{0.4}Sb$ layers with the larger lattice constant contract as a result of biaxial compressive stress, whereas the InAs layers with the smaller lattice constant expand due to a biaxial tensile stress. The presence of the strain leads to the change of the energy band structure. The valence band of $Ga_{0.6}In_{0.4}Sb$ is overlapping the conduction band of InAs by approximately 100 meV, forming a staggered structure, with the electron-confinement in InAs and hole-confinement in $Ga_{0.6}In_{0.4}Sb$ at thermal equilibrium. Since the direction of the strain-induced polarization macroscopically depends on the orientation of the dipoles formed by the displacement of the cations and anions under the strain, the piezoelectric field which is proportional to the polarization is expected to have equal strength but opposite direction in A-face (cation is on the top surface) and B-face (anion is on the top surface) <311> superlattices.

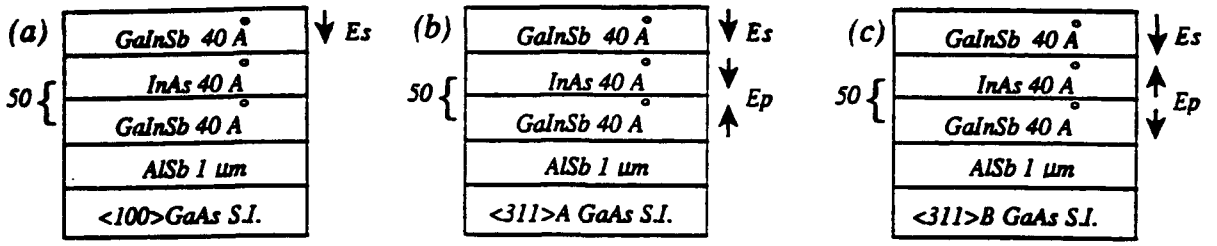

Figure 13. The schematic structures of $Ga_{0.6}In_{0.4}Sb$/InAs superlattices.

In contrast with the GaSb/AlSb superlattice of which AlSb is an indirect bandgap material, both the constituent layers of the GaInSb/InAs superlattice are direct bandgap materials. Due to the AlSb buffer which has lattice constant between that of $Ga_{0.6}In_{0.4}Sb$ and InAs, $Ga_{0.6}In_{0.4}Sb$ and InAs have opposite-oriented piezoelectric fields. The absorption coefficient of $Ga_{0.6}In_{0.4}Sb$ is about 3 times larger than that of InAs, resulting in over 200 times the carriers absorbed in $Ga_{0.6}In_{0.4}Sb$ layers than in InAs layers, and the $Ga_{0.6}In_{0.4}Sb$ layer suffers more strain due to more lattice distortion than InAs on a thick AlSb buffer. If the piezoelectric coefficients from $Ga_{0.6}In_{0.4}Sb$ and InAs are of the same order, the radiated signal from the $Ga_{0.6}In_{0.4}Sb$ layers will override the signal from the InAs layers.

For a zincblende strained-layer superlattice, a <100> or <110> oriented sample does not have a strain-induced piezoelectric field; the only static electric field is the surface depletion field. Superlattices with other orientations have the strain-induced piezoelectric field. The radiation from a <311> oriented superlattice has contributions both from the surface depletion field and from the piezoelectric field, whereas the radiation from a <100> oriented superlattice has a contribution only from the surface depletion field.[4] The waveforms of the optically induced radiation from three samples are plotted in Figure 14. The signal radiated from the <311>A sample clearly shows an opposite polarity compared with that from the <311>B sample. The amplitude of the signal from sample <311>A is smaller than that from sample <311>B, due to the surface depletion field

cancellation. If we assume the amplitude of the radiated signals is porportional to the internal field, the detected signal S, which is proportional to the radiated field, can be written as:

$$S_{<100>} = S(\vec{E}_s)$$
$$S_{<311>A} = S(\vec{E}_s) - S(\vec{E}_p)$$
$$S_{<311>B} = S(\vec{E}_s) + S(\vec{E}_p)$$

where $\vec{E}_s$ is the surface depletion field, which does not strongly depend on the crystal orientation, and $\vec{E}_p$ is the average macroscopic piezoelectric field in $Ga_{0.6}In_{0.4}Sb$ layers. The amplitudes of radiated signals from the surface depletion field and piezoelectric field can be further expressed by the measured signals from three samples $S_{<100>}$, $S_{<311>A}$ and $S_{<311>B}$ as:

$$S(\vec{E}_s) = S_{<100>} = \frac{1}{2}(S_{<311>A} + S_{<311>B})$$
$$S(\vec{E}_p) = \frac{1}{2}(S_{<311>B} - S_{<311>A})$$

The peak amplitudes of the waveforms in Figure 14 have the values $S_{<100>} = 0.35$, $S_{<311>A} = -0.5$, and $S_{<311>B} = 1.2$, separately. These measured data fit exactly with the foregoing equations. The good agreement between the experimental data and the calculated result suggests that the <311>A and <311>B oriented superlattice samples are of very high quality.

(a)

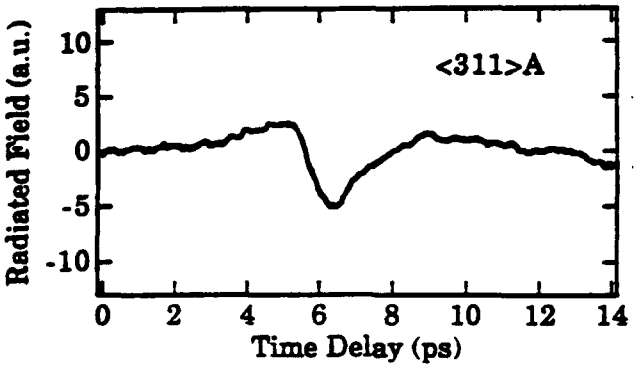

(b)

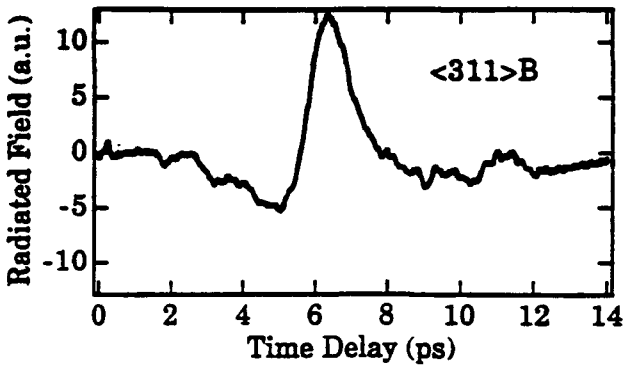

(c)

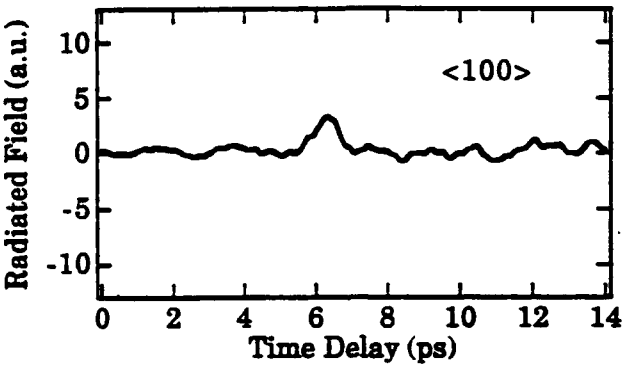

Figure 14. Waveforms of optically-induced electromagnetic radiation from <311>A, <311>B and <100> oriented $Ga_{0.6}In_{0.4}Sb$/InAs superlattices. The waveform from the <311>A oriented superlattice is opposite to the others due to the piezoelectric field in <311>A oriented superlattice being opposite to the <311>B oriented superlattice and the surface depletion field in the cap layer.

The $Ga_{0.6}In_{0.4}Sb$/InAs superlattices used here are not intentionally doped; Hall measurements show that samples are weakly p-type. Using the direction of the surface depletion field which points inward to the substrate as a reference to calibrate the field orientation, we find that the piezoelectric field in $Ga_{0.6}In_{0.4}Sb$ layers (not including the cap layer) is antiparallel to the surface depletion field in the <311>A sample and parallel in the <311>B sample. Due to the opposite direction of the piezoelectric field in the alternative layer, a vis-a-vis result can be achieved in the InAs layers of $Ga_{0.6}In_{0.4}Sb$/InAs superlattices. Following a similar analysis, this technique can be also extended to probe the field in other crystal orientations.

We have also tested the radiated signals from several <111> oriented GaSb/AlSb superlattices. The data from the <111> GaSb/AlSb superlattices, similar to the <311> GaInSb/InAs superlattices, showed an opposite polarity between the A-face and the B-face

samples, but their amplitudes did not agree with our analysis. This was perhaps due to the different sample quality, although they were grown under the same growth condition.

A key question that remains to be answered is the identification of the physical mechanism for the terahertz radiation. As mentioned earlier, it is possible that an important contribution to the signals could come from a virtual depolarization current, even when the photon energy is well above band gap. Our measurments in the strained layer superlattices seem to be consistent with this possibility. At the very high fields in these structures, we would expect the real drift currents to be saturated. Also, the size of the wells is too short for a well established drift current to develop, so that on this time scale, the signals may be due primarily to a virtual depolarization effect. Further measurements in samples where the field can be carefully controlled are necessary to resolve this issue.

References:

1. J. I. Pankove, Optical Processes in Semiconductors, ch 18, Dover Publications, Inc. New York (1975).

2. X.-C. Zhang, B. B. Hu, J. T. Darrow and D. H. Auston, Appl. Phys. Lett. **56**, 1011 (1990).

3. X.-C. Zhang, B. B. Hu, J. T. Darrow, S. H. Xin and D. H. Auston, Spring Series in Chemical Physics **53**, 198 (1990).

4. X.-C. Zhang, B. B. Hu, J. T. Darrow, S. H. Xin and D. H. Auston, Spring Series in Chemical Physics **53**, 198 (1990).

5. X.-C. Zhang, B. B Hu, X. H. Xin and D.H. Auston, Appl. Phys. Lett. **57**, 753, (1990).

6. X.-C. Zhang, J. T. Darrow, B. B. Hu, D. H. Auston, M. T. Schmidt, P. Tham and E.S. Yang, Appl. Phys. Lett. **56**, 2228 (1990).

7. S. L. Chuang, S. Schmitt-Rink, B. I. Greene, P. N. Saeta, and A.F.J. Levi, Phys. Rev. Lett. **68**, 102 (1992).

8. M. Yamanishi, Phys. Rev. Lett. **59**, 1014 (1987); D.S. Chemla, D.A.B. Miller, and S. Schmitt-Rink, Phys. Rev. Lett. **59**, 1018 (1987); E. Yablonovitch, J.P. Heritage, D.E. Aspnes, and Y. Yafet, Phys. Rev. Lett. **63**, 976 (1989); Y. Yafet, E. Yablonovitch, Phys. Rev. B **43**, 12480 (1991).

9. B. B. Hu, X.-C. Zhang and D. H. Auston, Phys. Rev. Lett. **67**, 2709 (1991).

10. B. B Hu, J. T. Darrow, X.-C. Zhang, D. H. Auston and P. R. Smith, Appl. Phys. Lett. **56**, 886 (1990).

11. P. R. Smith, D. H. Auston, and M. C. Nuss, IEEE J. Quantum Electron. **24**, 255 (1988).

12. Ch. Fattinger and D. Grischkowsky, Appl. Phys. Lett. **54**, 490 (1989).

13. B. B Hu, X.-C. Zhang, D. H. Auston and P. R. Smith, Appl. Phys. Lett. **56**, 506 (1990).

14. B. I. Greene, J. F. Federici, D. R. Dykaar, R. R. Jones and P. H. Buksbaum, Appl. Phys. Lett. **59**, 893 (1991).

15. G. M. Wysin, D. L. Smith, and A. Redondo, Phys. Rev. B **38**, 514 (1988).

16. D. L. Smith, Solid State Commun. **57**, 919 (1986).

17. D. L. Smith and C. Mailhiot, Rev. Mod. Phys. **62**,173 (1990).

18. B. K. Laurich, K.Elcess, C. G. Fonstad, J. G. Berry, C. Mailhiot and D. L. Smith, Phys. Rev. Lett. **62**, 649 (1989).

19. E. A. Caridi, T. Y. Chang, K. W. Goossen and L. F. Eastman, Appl. Phys. Lett. **56**, 659 (1990).

20. K. W. Goossen, E. A. Caridi, T. Y. Chang, J. B. Stark, D.A.B. Miller and R. A. Morgan, Appl. Phys. Lett. **56**, 715 (1990).

C. FUNDAMENTALS OF PROCESSING GAS/SURFACE INTERACTIONS

1. Quantum State-Resolved Studies of Gas/Surface Chemical Reactions (G. Flynn)

Our efforts over the past five years have been aimed at the detection of chlorine atoms and studies of their chemical reactions; the production and detection of hot electron/molecule collisions by a novel new technique; and a new effort to use lasers and laser photochemistry to enhance the sensitivity and selectivity of scanning tunneling microscopy. These experiments are providing data of fundamental interest for polymer etching, semiconductor surface etching and preparation, and plasma etching environments.

a. Chemical Dynamics of the Reaction between Chlorine Atoms and Deuterated Cyclohexane: We have studied the reaction of Cl atoms produced by excimer laser photolysis of NOCl precursor molecules:

$$NOCl + h\nu\ (193\ nm) \rightarrow Cl + NO \qquad (1)$$

This precursor produces Cl atoms with an average translational energy estimated to be approximately 16.4 kcal/mole (0.8 eV). The chlorine atoms then react with C_6D_{12} to form DCl:

$$Cl + C_6D_{12} \rightarrow C_6D_{11} + DCl \qquad (2)$$

DCl products are probed by time-resolved infrared absorption spectroscopy with a high resolution (~0.0003 cm^{-1}) lead-salt tunable diode laser:

$$DCl\ (v,J,V) + h\nu\ (\sim 4.9\ \mu m) \rightarrow DCl\ (v\pm1, J\pm1, V) \qquad (3)$$

where v,J, and V are the vibrational quantum number, rotational quantum number, and translational velocity, respectively.

We showed that Cl atoms with either 0.4 eV or 0.8 eV of energy give cold DCl rotational distributions with hot translational energy distributions (large DCl recoil). Most of the energy of the Cl atoms goes into the translational recoil of the DCl and not into the rotational or vibrational degrees of freedom.

These results clearly represent nonstatistical partitioning of energy into rotationally cold, but translationally hot DCl molecules. The data strongly suggests a direct abstraction mechanism with a collinear C....D....Cl recoil geometry for the transition state. The Cl atom does not necessarily have to approach in a linear configuration; even with non-collinear approach, a very small motion of the light D atom can produce a collinear transition state which then rapidly falls apart.

The observation of such a simple mechanism for a reaction between a large gas phase molecule and an atom raises the question as to whether reactions between atoms and thin film surface polymers might also exhibit similar behavior. Efforts to answer this and other questions regarding the reactivity of Cl atoms are continuing in our laboratory.

b. Photoproduction and Scattering of Hot Electrons: We have recently discovered a simple method for producing hot electrons and studying their collisions with molecules in the gas phase. A key and novel feature of the experiments is the resolution, $0.0003 cm^{-1}$ or approximately 4×10^{-8} eV! This compares with standard electron scattering experiments which have a typical energy resolution of about 80 cm^{-1} or 10 meV. The high resolution is obtained by observing the molecular collision partner rather than the scattered electron as is normal in most electron scattering experiments. Such studies can provide fundamental insight into the mechanisms and processes which are important in plasma etching reactors. Considerable interest in this technique has been exhibited by scientists working on plasma etching diagnostics at the IBM East Fishkill facility.

In brief the method is as follows: Electrons are produced in a pulse by two photon excimer laser photoionization of I_2 molecules.

$I_2+h\nu(193\ nm)\rightarrow I_2(D)$ $\quad\quad$ $I_2(D)+h\nu(193\ nm)\rightarrow I_2^+ + e(0\text{-}3\ eV)$

The electrons then collide with other species in the sample, producing vibrationally excited molecules,

$e+M\rightarrow M(v,J,V)+e$

where v denotes the level of vibrational excitation, J the level of rotational excitation, and V the velocity recoil of species M. The M(v,J,V) species are detected using infrared diode laser radiation having a frequency purity of 0.0003 cm^{-1}. A brief summary of the results obtained so far in the study of a variety of collision partners M is as follows: The electron imparts essentially no angular momentum or translational recoil to the molecule. In essence, the electron is so light that at the energies available in this particular experiment (0-3 eV), it cannot impart any significant momentum to the heavy M species. Vibrational energy is quite another matter, however. We find that all vibrational modes are excited efficiently. The relatively high efficiency of exciting vibrational states is due to the strong interaction of the electron with the molecular electronic structure.

We have also constructed an apparatus to measure directly the electron "pressure" in these experiments using a simple axial magnetic field and a pick-up coil around the sample cell. When the laser photoionizes the I_2, the electrons so produced exclude magnetic flux from the center region of the sample tube. This produces a detectable electronic signal in the pick-up coil wrapped around the cell. We have measured the current induced in such a coil when photoionization occurs. The signal shows both production and cooling of the electrons and can be used to determine electron density. Such a measurement is necessary in order to obtain cross sections for

electron excitation of molecules, a parameter of key interest to scientists at the IBM East Fishkill facility working on the fundamental physical processes of importance in plasma etching reactors.

c. Scanning Tunneling Microscopy and Laser Photochemistry: During the past year an exploratory research program involving the scanning tunneling microscope (STM) and its application to imaging molecular systems and novel materials was begun. A substantial portion of these initial efforts have been concerned with the characterization of highly conducting organic materials based on charge transfer salts. These have included both materials in traditional single crystal form and those fabricated as thin films using recently developed vacuum evaporation techniques. There is significant potential for the STM to contribute in the characterization of these materials, especially in the case of those fabricated as thin films. This is due to the ease of sample preparation and the capability of the STM to examine only the local surface electronic properties and structure. In addition, the STM is unique in its ability to ascertain both the presence of defects and the effects of doppant molecules on the atomic scale. Research in the area of organic charge transfer systems is very active due to the potential application of these materials in electronic and optical device fabrication, as well as in attempts to develop new and better superconducting materials. In our work, thin films formed from the donor molecule tetrathiafulvalene (TTF) and iodine have been studied. These films are fabricated on freshly cleaved mica substrates using a vacuum co-deposition technique similar to that described recently in the literature. A similar study of crystals of a charge transfer complex formed from a new donor molecule, dimethyltetrathiatetracene (DMTTT), with the well known acceptor molecule tetracyanoquinodimethane (TCNQ) also yielded interesting structural details.

One particular long term goal of this effort is to develop STM techniques in which molecules adsorbed on surfaces and other surface features could be "labeled" via their optical response. Our efforts in these studies are aimed at improving techniques for using scanning tunneling microscopy to image molecules which can be adsorbed on or bonded to surfaces such as highly ordered pyrolitic graphite (HOPG) and crystalline gold films which have well known

surface structures that can be easily characterized using the STM. In particular we are testing methods using light emitted from the adsorbates (induced by scattering via the tunnel electrons) to "brighten" the adsorbate image. Such an approach will take advantage of our expertise with optical techniques and photon detection and our knowledge of relaxation processes, which inevitably play a critical role in any luminescence experiment. Improved methods of imaging large molecules adsorbed on surfaces offer the possibility of determining structure and conformation in a rapid and simple manner. In addition, if this approach is successful, it will greatly enhance the potential to observe and identify chemical reactions occurring on both conducting and semiconducting surfaces.

The experimental program which we have undertaken involves the "wedding" of established optical experimental methods with the scanning tunneling microscope. Our primary objective in the development of these new experimental techniques is the identification and characterization of adsorbed molecules on well studied surfaces. The main thrust of this program is the spatially resolved collection and spectral analysis of light (luminescence) emanating from the tunneling junction of an operating STM, where the excitation of optically emitting adsorbate states has been induced by "collisions" with the tunnel electrons. These tunneling electrons interact strongly with tip-induced localized plasmon modes, and thus the overall photon emission is greatly enhanced as compared to more traditional electron induced photoemission experiments. The information contained in the optical signals, combined with the extremely high spatial resolution of the STM, will provide molecular imaging capabilities which are superior to ordinary STM experiments. A key feature of these experiments is the use of optical methods to enhance or "brighten" the image of the adsorbates by light emission or absorption while at the same time maintaining superb spatial resolution via the STM. Because the tunneling process is highly localized to a region of the surface which is the dimension of an atom, the inelastic electron scattering that leads to photon emission is similarly localized. Thus, photon emission can be directly correlated with a region of the surface which is of atomic or molecular dimension. Previous optical/STM studies have largely concentrated on metal and semiconductor surfaces, and

only recently have experiments been reported for thin copper phthalocyanine films. The indications from these reported experiments are that reasonable photon emission fluxes can be obtained with nanometer spatial resolution using typical STM operating conditions.

2. Photochemical and Photophysical Probes of Interfaces (N.Turro)

The research program supported by this ONR grant has explored the use of photochemical processes which can serve as probes to characterize the structure and dynamics of reactions which occur at a variety of interfaces. Interfacial chemistry is critical to many aspects of the microelectronics' industry and for the development of new materials and the development of novel nanostructures. Accordingly, we have emphasized investigation of fundamental processes that will reveal global, fundamental principles which are likely to have a general impact on the field. The accomplished research has involved: (1) studies of the modification of photochemical reactivity of ketones adsorbed on the internal surfaces on zeolites; (2) studies of the structure dependent photoinduced electron transfer between cations adsorbed on the surface of polyelectrolytes; and, (3) studies of the conformation of polymers adsorbed on solid interfaces.

The photolysis of aryl alkyl ketones adsorbed on the surface of faujasite zeolites has been shown to be controlled by the nature of the exchangeable compensating cations associated with a framework of the internal surface of the zeolite.[1] In a related study, the photochemistry of α-alkyldibenzyl ketones adsorbed on the internal surface of zeolites has been shown to depend on the exchangeable cation.[2] Photolysis of macrocylic mono and diketones adsorbed in faujasite zeolite have been shown to yield products resulting from cleavage of the α-carbon bond, which are not observed in isotropic media.[3] The reaction has been shown to be dependent on the nature of the charge compensating cation associated with the zeolite framework. These results represent a novel form of catalysis in which a reaction may be "tuned" by changing cations which behave as catalytic spectators for specific reaction pathways.

One of the first examples of bimolecular photochemical reactions of organic molecules adsorbed on the internal surface of zeolites, the dimerization of acenaphthylene, was investigated by both product analysis and time resolved laser flash photolysis.[4] The ratio of dimers formed was found to depend on the type of cation present in the supercage, in analogy to the cation dependence of the photolyses of ketones. Dimerization is proposed to originate from the excited singlet state for lower atomic number cations and from the triplet state in the case of higher atomic number cations. The results were employed to deduce the distribution and migration of molecules within the zeolite internal surface.

In addition to the photochemical investigation of "dry" systems, it has been found that zeolite-solvent systems are convenient for the control of photoreactions, both intermolecular and intramolecular.[5] The occurrence of solvent in the supercages of faujasites provides constraints on the mobility of the included guest molecules, which, in turn, controls the difference in the product distribution. These results add still another dimension to the control of reactions on porous solids.

The investigation of photoinduced electron transfer between a donor and acceptor pair adsorbed on the surface of the novel particles, starburst dendrimers, has been investigated in detail.[6] The electron transfer event was found to depend on the size of the dendrimer, whose diameter was systematically varied from 60 Å to 200 Å. The increase in size is accompanied by a decrease in the rate constant for electron transfer. It was also demonstrated that a similarity exists between the behavior of the electron transfer on dendrimers and micellar aggregates.

A novel phosphorescence probe of polymer conformation and interpolymer interactions was synthesized.[7] The phosphorescence lifetime was found to be pH dependent, dependent on the inclusion of complementary polymers, and dependent on the conformations of the polymer adsorbed on a solid-liquid interface.

The conformation of polyacrylic acid adsorbed on alumina has been investigated simultaneously with various flocculation properties by employing a spectroscopic fluorescence probe technique.[8] The results show that polymer conformation is a controlling factor of the

flocculation process. Under fixed pH conditions, the stretched polymer (which dangles into the liquid at the solid/liquid interface) gives better flocculation than the coiled polymer (which sites at the interface).

The adsorption of cations to a polyelectrolyte such as DNA has been investigated by time resolved luminescence.[9] The mechanism and nature of binding has been shown to be a rational function of the ligands associated with the cations.

The interaction of an anionic fluorescence probe has been employed to investigate the formation of micellar aggregates and premicellar aggregates.[10] It was shown that the interactions are a sensitive function of the complementary structures of the surfactant making up the micelle and the probe structure.

References:

1. V. Ramamurthy, D.R. Corbin, N.J. Turro and Y. Sato, "Modification of Photochemical Reactivity by Zeolites: Cation Enhanced α-cleavage of Aryl Alkyl Ketones Included in Faujasites," Tetrahedron Letters **30**, 5829 (1989).

2. V. Ramamurthy, D.R. Corbin, D.F. Eaton and N.J. Turro, "Modification of Photochemical Reactivity by Zeolites: Role of Cations in Controlling the Behavior of Radicals Generated within Faujasites," Tetrahedron Letters **30**, 5833 (1989).

3. V. Ramamurthy, X.-G. Lei, N.J. Turro, T.J. Lewis and J. R. Scheffer, "Photochemistry of Macrocyclic Ketones within Zeolites: Competition between Norrish Type I and Type II Reactivity," Tetrahedron Letters **32**, 7675 (1991).

4. V. Ramamurthy, D. R. Corbin, C. V. Kumar and N. J. Turro, "Modification of Photochemical Reactivity by Zeolites: Cation Controlled Photodimerisation of Acenaphthylene within Faujasites," Tetrahedron Letters **31**, 47 (1990).

5. V. Ramamurthy, D. R. Corbin, N. J. Turro, Z. Zhang, and M. A. Garcia-Garibay, "A Comparison between Zeolite-Solvent Slurry and Dry Solid Photolyses," J. Organic Chem. **56**, 255 (1991).

6. K. R. Gopidas, A. R. Leheny, G. Caminati, N. J. Turro and D. A. Tomalia, "Photophysical Investigation of Similarities between Starburst Dendrimers and Anionic Micelles," J. Am. Chem. Soc. **113**, 7335 (1991).

7. N.J. Turro, G. Caminati and J. Kim, "Photophorescence from a Bromonaphthalene Lumophore as a Photophysical Probe of Polymer Conformation and Interpolymer Interactions," Macromolecules **24**, 4054 (1991).

8. K. F. Tjipangandara, Y-B Huang, P. Somasundaran and N.J. Turro, "Correlation of Alumina Flocculation with Adsorbed Polyacrylic Acid and Conformation," Colloids and Surfaces **44**, 229 (1990).

9. A. Kirsch-De Mesmaeker, G. Orellana, J. K. Barton and N. J. Turro, "Ligand-Dependent Interaction of Ruthenium (II) Polypyridyl Complexes with DNA Probed by Emission Spectroscopy," Photochem. Photobiol. **52**, 461 (1990).

10. S. Niu, K. R. Gopidas, N. J. Turro, and G. Gabor, "Formation of Premicellar Clusters Between 2,6-Toluidine Naphthalenesulfonate with Cationic Detergents," Langmuir **8**, 1271 (1992).

III. PUBLICATIONS

1986-87

S. S. Todorov, C. F. Yu, and E. R. Fossum, "Direct Formation of Dielectric Films on Silicon by Low Energy Ion Beam Bombardment," Vacuum **36**, 929 (1986).

R. M. Osgood, Jr. "An Overview of Laser Chemical Processing," Proc. of the Mat. Res. Soc. Symp. A and B **74**, 75 (1987).

C. F. Yu, S. S. Todorov, and E. R. Fossum, "Characterization of Thin SiO_2 Films Formed by Direct Low Energy Ion Beam Oxidation," J. Vac. Sci. Technol. A **5**, 1569 (1987).

C. F. Yu, M. T. Schmidt, D. V. Podlesnik, and R. M. Osgood, Jr., "Wavelength Dependence of Optically Induced Oxidation of GaAs (100)," J. Vac. Sci. Technol. B **5**, 1087 (1987).

1988

J. A. O'Neill, J. Y. Cai, C. X. Wang, G. W. Flynn, and R. E. Weston, Jr., "Rotational Profiles of the 00^01 and 00^02 CO_2 States Produced by Collisions with Hot Hydrogen Atoms: A Diode Laser Probe Study," J. Chem. Phys. **88**, 6240 (1988).

M. H. Alexander, P. Andresen, R. Bersohn, *et.al.*, "A Nomenclature for the Asymmetry of λ Doublets in Linear Molecules," J. Chem. Phys. **89**, 1749 (1988).

T. G. Kreutz and G. W. Flynn, "Understanding the Dynamic Behavior of Molecular Vibrational States," Advances in Laser Science-III, Optical and Engineering Series **9**, AIP Conference Proceedings No. 172, A.C. Tam, J. L. Gole, and W. C. Stwalley, Eds., pp 280-289 (1988).

J. Hershberger, S. Hewitt, G. Flynn, and R. E. Weston, Jr., "Observation of an Odd/Even Delta-J Propensity In the Collisional Excitation of CO_2 by Hot Deuterium Atoms," J. Chem. Phys. **88**, 7243 (1988).

J. Hershberger, J. Chou, G. Flynn, and R. E. Weston, Jr., "Rotational State Dependence of Transient Linewidths in the CO_2 (00^01) Vibrational Level Due to Translational Energy Recoil from Hot H and D Atom Collisions," Chem. Phys. Lett. **149**, 51 (1988).

F. Khan, T. Kreutz, L. Zhu, G. Flynn, and R. E. Weston, Jr., "Temperature Dependence of Rotationally Resolved Excitation of $CO_2(00^01)$ by Collisions with Hot Hydrogen Atoms," J. Phys. Chem. **92**, 6170 (1988).

R. W. Ade and E. R. Fossum, "Fabrication of Epitaxial GaAs/AlGaAs Diaphragms by Selective Dry Etching," J. Vac. Sci. Technol. B **6**, 1592 (1988).

S. S. Todorov and E. R. Fossum, "Growth Mechanism of Thin Oxide Films Under Low-Energy Oxygen-Ion Bombardment," J. Vac. Sci. Technol. B **6**, 466 (1988).

G. D. Pazionis, H. Tang, L. Ge, and I. P. Herman, "Stokes/Anti-Stokes Raman Microprobe Analysis of Laser-Heated Silicon Microstructures on Silicon Dioxide," Mat. Res. Soc. Symp. Proc. **101**, 113 (1988).

D. E. Kotecki and I. P. Herman, "A Real-Time Monte Carlo Simulation of Thin Film Nucleation in Localized-Laser Chemical Vapor Deposition," J. Appl. Phys. **64**, 4920 (1988).

D. E. Kotecki and I. P. Herman, "Initial Stages of Silicon Growth on the (100) Surface of Silicon by Localized Laser CVD," Mat. Res. Soc. Sym. Proc. **101**, 119 (1988).

L. P. Welsh, J. A. Tuchman, and I. P. Herman, "The Importance of Thermal Stresses and Strains Induced in Laser Processing with Focused Gaussian Beams," J. Appl. Phys. **64**, 6274 (1988).

M. T. Schmidt, C. F. Yu, D. V. Podlesnik, E. S. Yang and R. M. Osgood, Jr., "Schottky Contact Characterization of Thin Excimer Laser Grown GaAs Oxides," MRS Symposium Proc. **101**, 421 (1988).

A. E. Willner, O. J. Glembocki, D. V. Podlesnik, E. Palik, and R. M. Osgood, Jr., "Surface Potential Characterization of the Photochemical Etching System by Photoreflectance and Electroreflectance Technique," SPIE Symp. Proc. **946**, 48 (1988).

M. T. Schmidt, C. F. Yu, Z. Wu, D. V. Podlesnik, E. S. Yang, and R. M. Osgood, Jr., "Ultraviolet Laser Induced Photochemistry on GaAs surfaces," Proc. of the American Vacuum Society National Symp., Atlanta, Georgia, (October 1988).

M. T. Schmidt, D. V. Podlesnik, C. F. Yu, E. S. Yang, R. M. Osgood, Jr., "*In Situ* Processing for GaAs Devices Using Ultraviolet Formed Oxides," Cong. on Lasers and Electro-Optics Techn. Digest (Opt. Soc. of Amer., Washington, D. C. 1988): 286.

M. T. Schmidt, D. V. Podlesnik, H. L. Evans, C. F. Yu, E. S. Yang, and R. M. Osgood, Jr., "The Effect of a Thin Ultra-Violet Grown Oxide on Metal-GaAs Contacts," J. Vac. Sci. Technol. A **6**, 1446 (1988).

C. F. Yu, M. T. Schmidt, D. V. Podlesnik, E. S. Yang, and R. M. Osgood, Jr., "Ultraviolet-Light-Enhanced Reaction of Oxygen with Gallium Arsenide Surfaces," J. Vac. Sci. Technol. A **6**, 754 (1988).

L. Chen, V. Liberman, J. A. O'Neill, and R. M. Osgood, Jr., "Low-Coverage Laser Desorption of Ions on Chlorinated Copper Surfaces," MRS Symposium Proc. **101**, 463 (1988).

M. T. Schmidt, D. V. Podlesnik, C. F. Yu, X. Wu, R. M. Osgood, Jr., and E. S. Yang, "Increased Dependence of Schottky Barrier Height on Metal Work Function Due to a Thin-oxide Layer," J. Vac. Sci. Technol. B **6**, 1436 (1988).

D. V. Podlesnik, M. T. Schmidt, C. F. Yu, and R. M. Osgood, Jr., "Laser-Controlled Surface Modification of Semiconductors," Proc. of the 32nd International Symp. on Electron, Ion, and Photon Beams, Ft. Lauderdale, Florida, (1988).

E. Sanchez, P. S. Shaw, J. A. O'Neill and R. M. Osgood, Jr., "Infrared Total Internal Reflection Spectroscopy of Dimethylcadmium on Chemically Passivated Silicon Surfaces," Chem. Phys. Letts. **147**, 153 (1988).

T. Cacouris, G. Scelsi, P. Shaw, R. Scarmozzino and R. M. Osgood, Jr., "Laser Direct Writing of Aluminum Conductors," Appl. Phys. Lett. **52**, 1865 (1988).

E. Sanchez, P. Shaw, and J. A. O'Neill, "Infrared Total Internal Reflection Spectroscopy of DMCd on Silicon," J. Vac. Sci. Technol. A **3**, 765, (May 1988).

L. F. Luo, R. Beresford, and W. I. Wang, "Resonant Tunneling in AlSb/InAs/AlSb Double-barrier Heterostructures," Appl. Phys. Lett. **53**, 2320 (1988).

E. E. Mendez, E. Calleja, and W. I. Wang, "Inelastic Tunneling in AlAs/GaAs/AlAs Heterostructures," Appl. Phys. Lett. **53**, 977 (1988).

1989

B. B.Hu, X.-C. Zhang, D. H. Auston, "Femtosecond Electrical Pulses in Free Space," Proc. of Annual Meeting of the Optical Society of America (October, 1989).

J. Z. Chou, S. A. Hewitt, J. F. Hershberger, B. B. Brady, G. B. Spector, L. Chia, and G. W. Flynn, "Diode Laser Probing of the High Frequency Vibrational Modes of Baths of CO_2, N_2O and CO Excited by Relaxation of Highly Excited NO_2," J. Chem. Phys. **91**, 5392 (1989).

J. F. Hershberger, S. A. Hewitt, S. K. Sarkar, and G. W. Flynn, "Quantum State-Resolved Study of Pure Rotational Excitation of CO_2 by Hot Atoms," J. Phys. Chem. **91**, 4636 (1989).

G. W. Flynn, "Chemical Cartography: Finding the Keys to the Kinetic Labyrinth," Science **246**, 1009 (1989).

J. I. Song and E. R. Fossum, "Characterization of Evaporated Cr-SiO Cermet Films for Resistive Gate CCD Applications," IEEE Trans. Electron Devices **ED-36**, 1575 (1989).

R. E. Colbeth, D. V. Rossi, J. I. Song, and E. R. Fossum, "GHZ GaAs CCDs: Promises, Problems, and Progress," Proc. SPIE **1071**, 108 (1989).

R. E. Colbeth, J. I. Song, D. V. Rossi, and E. R. Fossum, "A Recessed-gap Capacitive Gate GaAs CCD," IEEE Electron Device Lett. **EDL-10**, 525 (1989).

R. E. Colbeth, J. I. Song, D. V. Rossi and E. R. Fossum, "A1 GHz GaAs CCD with Capacitive Gates and High Transfer Efficiency," Proc. 1989 International Symp. on VLSI Technology, Systems, and Applications, Taipei, Taiwan, (May 1989).

G. D. Pazionis, H. Tang, and I. P. Herman, "Raman Microprobe Analysis of Temperature Profiles in cw Laser Heated Silicon Microstructures," IEEE J. Quantum Electron. **25**, 976 (1989).

I. P. Herman, "Laser Deposition of Thin Films from Gas-Phase and Adsorbed Molecules," Chem. Rev. **89**, 1323 (1989).

H. H. Burke, I. P. Herman, V. Tavitian and J. G. Eden, "Laser Photochemical Deposition of Germanium-Silicon Alloy Thin Films," Appl. Phys. Lett **55**, 253 (1989).

J. A. Tuchman, L. P. Welsh, and I. P. Herman, "Thermally Induced Stresses and Strains in Laser Processing of Thin Films," Mat. Res. Soc. Symp. Proc. **130**, 333 (1989).

R. M. Osgood, Jr., Laser Chemical Processing for Microelectronics, ed. K. Gibbs and R. M. Osgood, Jr., Cambridge University Press (1989).

M. T. Schmidt, Q. Y. Ma, D. V. Podlesnik and R. M. Osgood, Jr., "Chemically Modified GaAs Schottky Barrier Variation," J. of Vac. Sci. and Technol. B **7**, 980 (1989).

V. Ramamurthy, D. R. Corbin, N. J. Turro and Y. Sato, "Modification of Photochemical Reactivity by Zeolites: Cation Enhanced α-Cleavage of Aryl Alkyl Ketones Included in Faujasites," Tetrathedron Letters **30**, 5829 (1989).

V. Ramamurthy, D. R. Corbin, D. F. Eaton, and N. J. Turro, "Modification of Photochemical Reactivity by Zeolites: Role of Cations in Controlling the Behavior of Radicals Generated Within Faujasites," Tetrahedron Letters **30**, 5833 (1989).

B. V. Shanabrook, O. J. Glembocki, D. A. Broido, and W. I. Wang, "Luttinger Parameters for GaAs Determined from the Intersubband Transitions in GaAs/AlGaAs Multiple Quantum Wells," Phys. Rev. B **39**, 3411 (1989).

R. Beresford, L. F. Luo, and W. I. Wang, "Negative Differential Resistance in AlGaSb/InAs Sngle-barrier Heterostructures at Room Temperature," Appl. Phys. Lett. **54**, 1899 (1989).

L. F. Luo, R. Beresford, W. I. Wang, and E. E. Mendez, "Inelastic Tunneling in (111)-oriented AlAs/GaAs/AlAs Double-barrier Heterostructures," Appl. Phys. Lett. **54**, 2133 (1989).

R. Beresford, L. F. Luo, and W. I. Wang, "Tunneling in Narrow Band Gap Semiconductors", Proc. of the Int. Conf. Narrow Gap Semiconductors and Related Materials, Gaithersburg, MD, (June, 1989).

R. Beresford, L. F. Luo, W. I. Wang, and E. E. Mendez, "Resonant Tunneling Through X-valley States in GaAs/AlAs/GaAs Single-barrier Heterostructures," Appl. Phys. Lett. **55**, 1555 (1989).

L. F. Luo, R. Beresford, W. I. Wang, and H. Munekata, "Heterojunction Field-effect Transistors Based on AlGaSb/InAs," Appl. Phys. Lett. **55**, 789 (1989).

R. Beresford, L. F. Luo, and W. I. Wang, "Resonant Tunneling of Holes in AlSb/GaSb/AlSb Double-barrier Heterostructures," Appl. Phys. Lett. **55** 694 (1989).

L. F. Luo, R. Beresford, and W. I. Wang, "Interband Tunneling in Polytype Heterostructures," Appl. Phys. Lett. **55**, 2023 (1989).

R. Beresford, L. F. Luo, and W. I. Wang, "Band Structure Engineering for Electron Tunneling in Heterostructures," Proc. of the IEEE Device Research Conference, MIT, (June 22, 1989).

R. Beresford, L. F. Luo, and W. I. Wang, "Interband Tunneling in Polytype Heterostructure for High Speed Devices" Proc. of the International Electron Device Meeting (IEDM), Washington, D.C., 547 (Dec. 1989).

Q. Y. Ma, X. Wu, M. T. Schmidt, E. S. Yang, and C.-A. Chang, "Interdiffusion Between Si Substrates and SYBaCuO Films," Physica C **162**, 607 (1989).

X. Wu, M. T. Schmidt, E. S. Yang, "Control of the Schottky Barrier Using an Ultrathin Interface Metal Layer," Appl. Phys. Lett. **54**, 268 (1989).

Q. Y. Ma, E. S. Yang and C.-A. Chang, "Rapid Thermal Annealing of YBaCuO Thin Films Deposited on $S1O_2$ Substrates," J. Appl. Phys. **66**, 1866 (1989).

Q. Y. Ma, E. S. Yang, G. V. Treyz, and C.-A. Chang, "Novel Method of Patterning YBaCuO Superconducting Thin Films," Appl. Phys. Lett. **55**, 896 (1989).

L. F. Luo, H. L. Evans, and E. S. Yang, "A Heterojunction Bipolar Transistor with Separate Carrier Injection and Confinement," IEEE Trans. Elec. Dev. **36**, 1844 (1989).

1990

B. B. Hu, X.-C. Zhang, D. H. Auston and P. R. Smith, "Free Space Radiation from Electro-Optic Crystal," Appl. Phys. Lett. **56**, 506 (1990).

B. B. Hu, J. T. Darrow, X.-C. Zhang , D. H. Auston and P. R. Smith, "Optically-steerable Photoconducting Antennas," Appl. Phys. Lett. **56**, 886 (1990).

X.-C. Zhang, B. B. Hu, J. T. Darrow, and D. H. Auston, "Generation of Femtosecond Electromagnetic Pulses from Semiconductor Surfaces," Appl. Phys. Lett. **56**, 1011 (1990).

B. B. Hu, X.-C. Zhang, and D. H. Auston, "Temperature Dependence of Femtosecond Electromagnetic Radiation from semiconductor Surfaces," Appl. Phys. Lett. **57**, 2629 (1990).

X.-C. Zhang, J. T. Darrow, B. B. Hu, D. H. Auston, M. T. Schmidt, P. Tham and E. S. Yang, "Optically Induced Femtosecond Electromagnetic Pulses from Semiconductor Surfaces," Appl. Phys. Lett. **56**, 2228 (1990).

X.-C. Zhang, B. B. Hu, S. H. Xin, and D. H. Auston, "Optically Induced Femtosecond Electromagnetic Pulses from GaAs/AlSb Strained-layer Superlattices," Appl. Phys. Lett. **57**, 753 (1990).

C. Shu, X.-C. Zhang, E. S. Yang and D. H. Auston, "Optoelectronic Generation of Time-Division-Multiplexed Ultrafast Bit Stream on a Coplanar Waveguide," Appl. Phys. Lett. **57**, 2897 (1990).

C. Shu, X.-C. Zhang, E. S. Yang and D. H. Auston, "Optoelectronic Generation and Detection of 80 Gbit/s pulse Train," IEDM Tech. Digest, 327 (1990).

D. H. Auston, "Probing Semiconductor Materials & Devices with Picosecond and Femtosecond Optical Pulses," Physics Today (January, 1990).

D. H. Auston, "Probing Semiconductors with Femtosecond Pulses," Physics Today, 46-54, (February, 1990).

X.-C. Zhang, B. B. Hu, J. T. Darrow, S. H. Xin, and D. H. Auston, "Optically Induced Femtosecond Electromagnetic Radiation From Semiconductor Surfaces," in Springer Series in Chemical Physics **53**, (1990).

C. Shu, B. B. Hu, X.-C. Zhang, P. Mei, and E. S. Yang, "Picosecond Photoconductive Response of Polycrystalline Silicon Thin Films," Appl. Phys. Lett. **57**, 64 (1990).

J. T. Darrow, B. B. Hu, X.-C. Zhang, and D. H. Auston, "Subpicosecond Electromagnetic Pulses from Large-Aperture Photoconducting Antennas," Opt. Lett. **15**, 323 (1990).

J. M. Hossenlopp, J. F. Hershberger, and G. W. Flynn, "Kinetics and Product Vibrational Energy Disposal Dynamics in the Reaction of Chlorine Atoms with D_2S," J. Phys. Chem. **94**, 1346 (1990).

T. G. Kreutz, F. A. Khan, and G. W. Flynn, "Inversion of Experimental Data to Generate State-to-State Cross Sections for Ro-Vibrationally Inelastic Scattering of CO_2 by Hot Hydrogen Atoms," J. Chem. Phys. **92**, 347 (1990).

F. A. Khan, T. G. Kreutz, G. W. Flynn, and R. E. Weston, Jr., "State Resolved Vibrational, Rotational, and Translational Energy Deposition in $CO_2(00^01)$ Excited by Collisions with Hot Hydrogen Atoms," J. Chem. Phys. **92**, 4876 (1990).

L. Zhu, T. G. Kreutz, A. S. Hewitt, and G. W. Flynn, "Diode Laser Probing of Vibrational, Rotational, and Translational Excitation of CO_2 Following Collisions with $O(^1D)$: Inelastic Scattering," J. Chem. Phys. **93**, 3277 (1990).

T. G. Kreutz and G. W. Flynn, "Analysis of Translational, Rotational, and Vibrational Energy Transfer in Collisions between CO_2 and Hot Hydrogen Atoms: The Three Dimensional 'Breathing Ellipse' Model," J. Chem. Phys. **93**, 452 (1990).

F. A. Khan, T. G. Kreutz, J. A. O'Neill, C. X.Wang, G. W. Flynn, and R. E. Weston, Jr., "Collisional Excitation of $CO_2(01^11)$ by Hot Hydrogen Atoms: Alternating Intensities in State Resolved Vibrational, Rotational, and Translational Energy Transfer," J. Chem. Phys. **93**, 445 (1990).

L. Zhu, J. Hershberger, and G.W. Flynn, "Quantum State Resolved Study of the Rovibrational Excitation of OCS by Hot Hydrogen Atoms," J. Chem. Phys. **92**, 1687 (1990).

S. A. Hewitt, L. Zhu, and G. W. Flynn, "Diode Laser Probing of the Asymmetric Stretch Mode of CO_2 Produced by Collisions with High Energy Electrons from 193 nm Excimer Laser Photolysis of Iodine," J. Chem. Phys. **92**, 6974 (1990).

J. Z. Chou and G. W. Flynn, "Energy Dependence of the Relaxation of Highly Excited NO_2 Donors Under Single Collision Conditions: Vibrational and Rotational State Dependence and Translational Recoil of CO_2 Quencher Molecules," J. Chem. Phys. **93**, 6099 (1990).

S. A. Hewitt, J. F. Hershberger, J. Z. Chou, G. W. Flynn, and R. E. Weston, Jr., "Rotationally and Translationally Resolved Hot Atom Collisional Excitation of the CO_2 Fermi Mixed Bend/Stretch Vibrational Levels By Time-Dependent Diode Laser Spectroscopy," J. Chem. Phys. **93**, 4922 (1990).

J. Z. Chou, S. A. Hewitt, J. F. Hershberger, and G. W. Flynn, "Diode Laser Probing of the Low Frequency Vibrational Modes of Baths of CO_2 and N_2O Excited by Relaxation of Highly Excited NO_2," J. Chem. Phys. **93**, 8474 (1990).

H. Tang and I. Herman, "Local Laser Induced Etching of Copper Films by Chlorine," Mat. Res. Soc. Symp. Proc. **158**, 331 (1990).

H. Tang and I. Herman, "Laser-induced and Room Temperature Etching of Copper Films by Chlorine with Analysis by Raman Spectroscopy," J. Vac. Sci. Technol. **A8**, 1608 (1990).

M. T. Schmidt, Z. Wu, C. F. Yu and R. M. Osgood, Jr., "Atomic Movement During the Oxidation of GaAs," Surface Science **226**, 199 (1990).

Z. Lu, M. T. Schmidt, D. V. Podlesnik, C. F. Yu and R. M. Osgood, Jr., "Ultraviolet-Light-Induced Oxide Formation on GaAs Surfaces," J. Chem. Phys. **93**, 7951 (1990).

Q. Y. Ma, E. S. Yang, G. V. Treyz, C. Shu, R. M. Osgood, Jr., and C.-A. Chang, "Use of Si-YBaCuO Intermixed System for Patterning of Superconducting Thin Films," Proc. of MRS 89 Fall Meeting, Boston, MA **169**, 1189 (1990).

T. J. Licata, M. T. Schmidt, D. V. Podlesnik, V. Liberman and R. M. Osgood, Jr., "The Formation of Elevated Barrier Height Schottky Diodes to InP and In0.47Ga0.53As Using Thin, Excimer Laser-Deposited Cd Interlayers," J. of Electron. Mat. **19**, 1239 (1990).

X. G. Zhang, J. S. Shor, M. N. Ruberto, M. T. Schmidt and R. M. Osgood, Jr., "Laser Electrochemical Etching of SiC," Proc. of the SOTAPOCS XII Symposium of the Electrochemical Society, Montreal, Canada **90-15**, 271 (1990).

V. Ramamurthy, D. R. Corbin, C. V. Kumar and N. J. Turro, "Modification of Photochemical Reactivity by Zeolites: Cation Controlled Photodimerization of Acenaphthylene within Faujasites," Tetrahedron Letters **31**, 47 (1990).

A. Kirsch-De Mesmaeker, G. Orellana, J. K. Barton and N. J. Turro, "Ligant-Dependent Interaction of Ruthenium (II)polypyridyl Complexes with DNA Probed by Emission Spectroscopy," Photochem. Photobiol. **52**, 461 (1990).

K. F. Tjipangandara, Y-B Huang, P. Somasundaran and N. J. Turro, "Correlation of Alumina Flocculation with Adsorbed Polyacrylic Acid and Conformation," Colloids and Surfaces **44**. 229 (1990).

W. Hansen, T. P. Smith, III, J. Piao, R. Beresford, and W. I. Wang, "Symmetry and Strain Effects in GaSb/AlSb Quantum Wells," Appl. Phys. Lett. **56**, 81 (1990).

K. F. Longenbach, L. F. Luo, and W. I. Wang, "Tunneling in Polytype InAs/AlSb/GaSb Heterostructures," Proc. of the NATO Advanced Workshop on Resonant Tunneling, Madrid, Spain, 41 (May 1990), .

K. F. Longenbach, L. F. Luo, and W. I. Wang, "Resonant Interband Tunneling in InAs/GaSb/AlSb/InAs and GaSb/InAs/AlSb/GaSb Heterostructures," Appl. Phys. Lett. **57**, 1554 (1990).

B. V. Shanabrook, D. Gammon, R. Beresford, W. I. Wang, R. P. Leavitt, and D. A. Broido, "Modification of the Piezoelectric Field in Quantum Wells," Proc. of the 20th International Conf.: Physics of Semiconductors, p. 901 World Scientific (1990).

L. F. Luo, K. F. Longenbach, and W.I. Wang, "P-channel Modulation-doped Field-effect Transistors Based on AlSbAs/GaAs," IEEE Trans. Electron Dev. **11**, 567 (1990).

B. V. Shanabrook, D. Gammon, R. Beresford, and W. I. Wang, "Optical Induced Variability of the Strain Induced Electric Fields and Band Structure in (111) GaSb/A1Sb Quantum Wells," Bull. Am. Phys. Soc. **35**, 572 (1990).

J. Piao, R. Beresford, and W. I. Wang, "Surface Structures of the AlGaSb System," J. Vac. Sci. Tech. B **8**, 276 (1990).

R. J. Wagner and W. I. Wang, "Hole Cyclotron Resonance in GaSb/AlSb Multiple Quantum Wells," Bull. Am. Phys. Soc. **35**, 825 (1990).

R. Beresford, L. F. Luo, and W. I. Wang, "Narrow Gap InAs for Heterostructure Tunneling," Semiconductor Science and Technology **5**, 195 (1990).

L. F. Luo, R. Beresford, K. F. Longenbach, and W. I. Wang, "Resonant Interband Coupling in Single-Barrier Heterostructures of InAs/GaSb/InAs and GaSb/InAs/GaSb," Appl. Phys. Lett. **68**, 2854 (1990).

R. Beresford, L. F. Luo, and W. I. Wang, "Resonant Interband Tunneling Device with Multiple Negative Differential Resistance Regions," IEEE Electron Dev. Lett. **11**, 110 (1990).

R. Beresford, L. F. Luo, and W. I. Wang, "Interband Tunneling Through Single Barrier InAs/AlSb/GaSb Heterostructures," Appl. Phys. Lett. **56**, 952 (1990).

R. Beresford, L. F. Luo, K. F. Longenbach, and W. I. Wang, "Resonant Interband Tunneling Through a 110 nm InAs Quantum Well," Appl. Phys. Lett. **56**, 551 (1990).

W. Hansen, T. P. Smith III, J. Piao, R. Beresford, and W. I. Wang, "Magnetoresistance Measurements of Doping Symmetry and Strain Effects in GaSb/AlSb Quantum Wells," Appl. Phys. Lett. **56**, 81 (1990).

X. Wu, Y. Q. Wang, E. S. Yang, "An AlGaAs/GaAs Heterostructure-Emitter Bipolar Transistor," IEEE Electron Device Lett. **II(6)**, 264 (1990).

Q. Y. Ma, M. T. Schmidt, E. S. Yang and C. A. Chang, "Processing and Substrate Effects on YBaCuO Thin Films Formed by Rapid Thermal Annealing of Cu/BaO/Y_2/O_3 Layered Structures," Superconductivity and Applications, Ed. H. S. Kwok et al., Plenum Press, NY pp. 175-183 (1990).

Q. Y. Ma and E. S. Yang, "Current Controlled High Tc Superconducting Switch," Cryogenics **30**, 1146 (1990).

X. Wu and E. S. Yang, "Effective Metal Screening and Schottky Barrier Formation in Metal-GaAs Structures," IEEE Dev. Lett. **11**, 315 (1990).

U. Gennser, V. P. Kesan, T. J. Bucelot, S. S. Iyer and E. S. Yang, "Resonant Tunneling of Holes Through Si Barriers," J. Vac. Sci. Technol **B-8**, 210 (1990).

X. Wu, E. S. Yang and N. D. Theodore, "Structural Characterization of Ti and Pt Thin Films on GaAs (110) Substrate," J. Electron. Materials **19**, 821 (1990).

X. Wu, E. S. Yang and H. L. Evans, "Negative Capacitance at Metal-Semiconductor Interfaces," J. Appl. Phys. **68**, 2845 (1990).

C. Shu, B. B. Hu, X.-C. Zhang, P. Mei, and E. S. Yang, "Picosecond Photoconductive Response of Polycrystalline Silicon Thin-films," Appl. Phys. Lett. **57**, 64 (1990).

M. T. Schmidt, Q. Y. Ma, L. S. Weinman, X. Wu, E. S. Yang, and C.-A. Chang, "Chemistry and Resistance at Metal Contacts to $YBa_2Cu_3O_7$ High T_c Superconducting Thin Films," American Inst. of Phys., 218 (1990).

1991

C. Shu, X. Wu, E. S. Yang, X.-C. Zhang and D. H. Auston, "Propagation Characteristics of Picosecond Electrical Pulses on a Periodically Loaded Coplanar Waveguide," IEEE Trans. Microwave Theory Tech. **30**, 930 (1991).

D. H. Auston and X.-C. Zhang, "Large-Aperture Photoconducting Antennas," OSA Proceedings on Picosecond Eectronics and Optoelectronics, 1991, Vol. 9. Gerhard Sollner and Jagdeep Shah (eds.)

B. B. Hu, X.-C Zhang and D. H. Auston, "Terahertz Radiation Induced by Sub-bandgap Femtosecond Optical Excitation," Phys. Rev. Lett. **67**, 2709 (1991).

L. Xu, X.-C. Zhang, D. H. Auston and W. I. Wang, " Internal Piezoelectric Field in Strained Layer GaInSb/InAs Superlattices Probed by Optically Induced Microwave Radiation," Appl. Phys. Lett. **59**, 3562 (1991).

N. M. Froberg, B. B. Hu, X.-C. Zhang, and D. H. Auston, "Time-division Multiplexing by a Photoconducting Antenna Array," Appl. Phys. Lett. **59**, 3207 (1991).

L. Xu, X.-C. Zhang, D. H. Auston and B. Jalali, "Terahertz Radiation from Large Aperture Si p-i-n Diode,"Appl. Phys. Lett. **56**, 3357 (1991).

P. Ferm, C. Knapp, C. Wu, J. Yardley, B. B. Hu, X.-C. Zhang, and D. H. Auston, "Femtosecond Response of the Electrooptic Poled Polymers," Appl. Phys. Lett **59**, 2651 (1991).

B. B. Hu, N. M. Froberg, M. Mack, X.-C. Zhang, and D. H. Auston, "Electrically-controlled Frequency Scanning by a Photoconducting Antenna Array," Appl. Phys. Lett. **58**, 1369, (1991).

N. M. Froberg, M. Mack, B. B. Hu, X.-C. Zhang, and D. H. Auston, "500 GHz Electrically Steerable Photoconducting Antenna Array," Appl. Phys. Lett. **58**, 446 (1991).

J. T. Darrow, X.-C. Zhang and D. H. Auston, "Power Scaling of Large-aperture Photoconducting Antennas," Appl. Phys. Lett. **58**, 25 (1991).

L. Zhu, S. A. Hewitt, and G. W. Flynn, "Quantum Interference Effects in the Collisional Excitation of the Fermi Doublet States of CO_2 by Hot Electrons and Hot H(D) Atoms," J. Chem. Phys. **94**, 4088 (1991).

L. Zheng, J. Chou, and G. Flynn, "Relaxation of Molecules with Chemically Significant Amounts of Energy: Vibrational, Rotational and Translational Energy Recoil of an N_2O Bath Due to Collisions with NO_2 (E=63.5 KCAL/MOLE)," J. Phys. Chem. **95**, 6759 (1991).

J. Park, Y. Lee, and G. Flynn, "Tunable Diode Laser Probe of Chlorine Atoms Produced from the Photodissociation of a Number of Molecular Precursors," Chem. Phys. Lett. **186**, 441 (1991).

H. Tang and I. P. Herman, "Raman Microprobe Scattering of Solid Silicon and Germanium at the Melting Temperature," Phys. Rev. B **43**, 2299 (1991).

Z. Sui, I. P. Herman, and J. Bevk, "Raman Analysis of Si/Ge Strained Layer Superlattices under Hydrostatic Pressure," Appl. Phys. Lett. **58**, 2351 (1991).

I. P. Herman, H. Tang, and P. P. Leong, "Real Time Optical Diagnostics in Laser Etching and Deposition," Mat. Res. Soc. Symp. Proc. **201**, 563 (1991).

Z. Sui, I. P. Herman, and J. Bevk, "Raman Study of Strain and Confinement Effects in Si/Ge Strained Layer Superlattices under Hydrostatic Pressure," Mat. Res. Soc. Symp. Proc. **220**, 333 (1991).

P. S. Shaw, E. Sanchez, J. A. O'Neill, Z. Wu and R. M. Osgood, Jr., "Surface Photochemistry of Divalent Metal Alkyls on SiO_2," J. Chem. Phys. Let. **94**, 1643 (1991).

M. T. Schmidt, Z. Wu and R. M. Osgood, Jr., "A Marker Technique to Identify Diffusing Elements During Initial Reactions Using Ion Spectroscopy," Surface and Interface Analysis **17**, 43 (1991).

T. J. Licata, M. T. Schmidt and R. M. Osgood, Jr., "The Application of Photodeposited Cd to Schottky Barrier Diode and MESFET Fabrication on InP and $In_{0.47}Ga_{0.53}As$ Substrates," Appl. Phys. Let. **58**, 845 (1991).

Z. Lu, M. T. Schmidt, D. L. Chen and R. M. Osgood, Jr., "GaAs-Oxide Removal Using an ECR Hydrogen Plasma," Appl. Phys. Lett. **58**, 1143 (1991).

Z. Lu, M. Schmidt and R. M. Osgood, Jr., "GaAs Surface Oxidation and Deoxidation Using Electron Cyclotron Resonance Oxygen and Hydrogen Plasmas," J. Vac. Sci. Technol. A **9**, 1040 (1991).

V. Liberman, G. Haase and R. M. Osgood, Jr., "Interaction of Cl_2 With GaAs(110) With and Without Laser Irradiation," Chem. Phys. Let. **176**, 379 (1991).

V. Ramamurthy, D. R. Corbin, N. J. Turro, Z. Zhang and M. A. Garcia-Garibay, "Modification of Photochemical Reactivity by Zeolites: A Comparison between Zeolite-Solvent Slurry and Dry Solid Photolyses," J. Org. Chem. **56**, 255 (1991).

N. J. Turro, G. Caminati and J. Kim, "Photophorescence from a Bromonaphthalene Lumophore as a Photophysical Probe of Polymer Conformation and Interpolymer Interactions," Macromolecules **24**, 4054 (1991).

K. R. Gopidas, A. R. Leheny, G. Caminati, N. J. Turro and D. A. Tomalia, "Photophysical Investigation of Similarities between Starburst Dendrimers and Anionic Micelles," J. Am. Chem. Soc. **113**, 7335 (1991).

V. Ramamurthy, X.-G. Lei, N. J. Turro, T. J. Lewis and J. R. Scheffer, "Photochemistry of Macrocyclic Ketones within Zeolites; Competition between Norrish Type I and Type II Reactivity," Tetrahedron Letters **32**, 7675 (1991).

L. F. Luo, K.F. Longenbach, and W. I. Wang, "P-channel Modulation-doped GaSb Field Effect Transistors," Electronics Lett. **27**, 472 (1991).

E. E. Mendez, H. Ohno, L. Esaki, and W. I. Wang, "Resonant Interband Tunneling via Landau Levels in Polytype Heterostructures," Phys. Rev. B **43**, 5196 (1991).

E. E. Mendez, H. Ohno, L. Esaki, and W. I. Wang, "Resonant Magnetotunneling in Type-II Heterostructures," Proc. NATO Advanced Workshop on Resonant Tunneling in Semiconductors: Physics and Applications, edited by L.L. Chang, E.E. Mendez, and C. Tejedor, Plenum, NY 1991.

K. F. Longenbach, L. F. Luo, and W. I. Wang, "Resonant Tunneling in Polytype InAs/AlSb/GaSb Heterostructures," Proc. NATO Advanced Workshop on Resonant Tunneling in Semiconductors: Physics and Applications, edited by L.L. Chang, E.E. Mendez, and C. Tejedor, Plenum, NY 1991.

K. F. Longenbach, L. F. Luo, S. Xin, and W. I. Wang, "Resonant Tunneling in Polytype InAs/AlSb/GaSb Heterostructures," J. Crystal Growth **111**, 651 (1991).

S. Xin. K. F. Longenbach, and W. I. Wang, "Low temperature Growth of GaAs Quantum Well Lasers by Modulated Beam Epitaxy," Electronics Lett. **27**, 1072 (1991).

K. F. Longenbach, S. Xin, C. Schwartz, Y. Jiang, and W. I. Wang, "Modulated Beam Epitaxial Growth of High Quality GaAs Single Quantum Wells at Low Temperature," Appl. Phys. Lett. **59**, 820 (1991).

K. F. Longenbach, S. Xin, C. Schwartz, Y. Jiang, and W. I. Wang, "Low Temperature Growth of High Quality GaAs Quantum Wells and Lasers by Modulated Beam Epitaxy," Proc. of the Spring Meeting of the Materials Research Society, Anaheim CA, 203 (May 1991).

K. F. Longenbach, S. Xin, and W. I. Wang, "p-type Doping of GaSb by Ge and Sn by Molecular Beam Epitaxy," J. Appl. Phys. **69**, 3393 (1991).

K. F. Longenbach, Y. Wang, and W. I. Wang, "Two-dimensional Electron Gas Modulated Resonant Tunneling Transistor," Appl. Phys. Lett. **59**, 967 (1991).

K. F. Longenbach, Y. Wang, and W. I. Wang, "A Two-dimensional Electron Gas Modulated Resonant Tunneling Transistor," Proc. of the 18th Int. Conf. on GaAs and Related Compounds, Seattle, WA, (Sept., 1991).

K. F. Longenbach and W. I. Wang, "AlGaSb/GaSb Diodes Grown by Molecular Beam Epitaxy," Appl. Phys. Lett. **59**, 1117 (1991).

K. F. Longenbach and W. I. Wang, "Molecular Beam Epitaxy of GaSb," Appl. Phys. Lett. **59**, 2427 (1991).

H. Xie, J. Piao, J. Katz, and W. I. Wang, "Intersubband Absorption in GaAlSb/AlSb Superlattices for Infrared Detection," J. Appl. Phys. **70**, 8152 (1991).

K. F. Longenbach, X. Li, Y. Wang, and W. I. Wang, "Polytype InAs/AlSb/GaSb for Field Effect Transistor Applications," Proc. IEEE/Cornell Conference on Advanced Concepts in High Speed Semiconductor Devices and Circuits, 270 (1991).

M. H. Kim, M. A. Plano, M. A. Haase, G. E. Stillman, and W. I. Wang, "Photo-Hall Studies of High Purity GaAs," J. Appl. Phys. **70**, 7425 (1991).

Q. Wang, Y. Wang, K. F. Longenbach, E. S. Yang, and W. I. Wang, "A two-dimensional Electron Gas Emitter AlGaAs/GaAs Heterojunction Bipolar Tansistor," Appl. Phys. Lett. **59**, 2582 (1991).

Y. Wang, Q. Wang, K. F. Longenbach, E. S. Yang, and W. I. Wang, "A Two-dimensional Electron Gas Emitter AlGaAs/GaAs Heterojunction with Low Offset Voltage," Proc. of 18th Int. Conf. on GaAs and Related Compounds, Seattle, WA, 311 (Sept. 1991).

Q. Y. Ma, M. T. Schmidt, L. S. Weinman, E. S. Yang, S. M. Sampere and S. W. Chan, "Characterization of Bi-Metal Contacts to High Tc Superconducting Films," J. Vac. Sci. Tech. A **9**, 390 (1991).

Q. Y. Ma, C. A. Chang and E. S. Yang, "Observation of Anomalous Resistance Transistion Around 160-200 K in $Y_5Ba_6Cu_{11}Ox$ Thin Films," J. Appl. Phys. **69**, 7348 (1991).

P. Mei, M. T. Schmidt, E. S. Yang, and B. J. Wilkens, "Structural Study of Tin and Carbon Co-Implanted Silicon," J. Appl. Phys. **69**, 8417 (1991).

U. Gennser, V. P. Kesan, S. S. Iyer, T. J. Bucelot, and E. S. Yang, "Temperature Dependent Transport Measurement on Strained Si/Si_{1-x} Ge_x Resonant Tunneling Devices," J. Vac. Sci. and Tech. B **9**, 2059 (1991).

U. Gennser, V. P. Kesan, D. A. Syphers, T. P. Smith, III, S. S. Iyer, and E. S. Yang, "Magneto-Transport Measurements on $Si/Si_{1-x}Ge_x$ Resonant Tunneling Structures," Proc. Symposium on Si MBE, MRS Spring Meeting (1991).

K. H. Liou, P. Mei, U. Gennser, and E. S. Yang, "Effects of Ge Concentration of SiGe Oxidation Behavior," Appl. Phys. Lett. **59**, 1200 (1991).

1992

J. T. Darrow, X.-C. Zhang, D. H. Auston, and J. D. Morse, "Saturation Properties of Large-aperture Photoconducting Antennas," IEEE J. Quantum Electron. **28** (1992).

X.-C. Zhang and D. H. Auston, "Optoeletronic Measurement of Semiconductor Surfaces and Interface with Femtosecond Optics," J. Appl. Phys. **71**, 326 (1992).

N. M. Froberg, B. B. Hu, X.-C. Zhang, and D. H. Auston, "Terahertz Radiation from a Photoconducting Antenna Array," invited paper, to be published in IEEE J. Quantum Electron. (October, 1992).

J. Park, Y. Lee, J. F. Hershberger, J. M. Hossenlopp, and G. W. Flynn, "Chemical Dynamics of the Reaction between Chlorine Atoms and Deuterated Cyclohexane," J. Am. Chem. Soc. **114**, 58 (1992).

Z. Sui, P. Leong, and I. P. Herman, "Raman Analysis of Light-Emitting Porous Silicon," Appl. Phys. Lett. **60**, 2086 (1992).

H. Tang and I. P. Herman, "Polarization Raman Microprobe Analysis of Laser Melting and Etching of Silicon," J. Appl. Phys. **71**, 3492 (1992).

J. A. Tuchman and I. P. Herman, "General Trends in Changing Epilayer Strains Through the Application of Hydrostatic Pressure," Phys. Rev. B **45**, 11929 (1992).

H. Tang and I. P. Herman, "Anomalous Local Laser Etching of Copper by Chlorine," Appl. Phys. Lett. **60**, 2164 (1992).

I. P. Herman, "Raman Scattering as an *in situ* Optical Diagnostic," SPIE **1594**, 298 (1992).

Z. Sui, P. P. Leong, I. P. Herman, G. S. Higashi and H. Temkin, "Analysis of the Structure of Porous Silicon by Raman Scattering," Mat. Res. Soc. Symp. Proc. (1992, in press).

Q. Wang, E. S. Yang, P. W. Li, Z. Lu, R. M. Osgood, and W. I. Wang, "Electron Cyclotron Resonance Hydrogen and Nitrogen Plasma Surface Passivation of AlGaAs/GaAs Heterojunction Bipolar Transistors," IEEE Electron Dev. Lett. **13**, 83 (1992).

P. W. Li, Q. Wang and E. S. Yang, "Chemical and Electrical Characterization of AlGaAs/GaAs HBTs Treated by ECR Plasmas," Appl. Phys. Lett. **60**, 1996 (1992).

Z. Lu, D. Chen and R. M. Osgood, Jr. "Study of Thermal Oxide Solid-State Reactions on GaAs Surfaces," Mat. Res. Soc. Symp. Proc. **238**, 263 (1992).

Z. Lu, Y. Jiang, W. I. Wang, M. C. Teich, and R. M. Osgood, "GaSb-oxide Removal and Surface Passivation Using Electron Cyclotron Resonance Hydrogen Plasma," J. Vac. Sci. Technol. B **10**, (1992).

E. E. Mendez, J. Nocera, and W. I. Wang, "Conservation of Momentum and its Consequences in Interband Resonant Tunneling," Phys. Rev. B (Feb. 15, 1992).

S. Niu, K. R. Gopidas, N. J. Turro and G. Gabor, "Formation of Premicellar Clusters in 2,6-Toluidine Naphthalenesulfonate with Cationic Detergents," Langmuir **8**, 1271 (1992).

J. J. Breen and G. W. Flynn, "STM Studies of the Synthetic Polypeptide: Poly-γ-benzyl-L-glutamate," J. Phys. Chem., to be published.

R. E. Weston, Jr. and G. W. Flynn, "Relaxation of Molecules with Chemically Significant Amounts of Energy: The Dawn of the Quantum State Resolved Era," Ann. Rev. Phys. Chem., to be published.

C. K. Ni and G. W. Flynn, "Correlation between Molecular Recoil and Molecular Orientation in Collisions of Symmetric Top Molecules with Hot Hydrogen Atoms," Chem. Phys. Lett., to be published.

S. A. Hewitt, L. Zhu, and G. W. Flynn, "Diode Laser Probing of CO_2 and CO Vibrational Excitation Produced by Collisions with High Energy Electrons from 193 nm Excimer Laser Photolysis of Iodine," submitted for publication.

F. A. Khan, T. G. Kreutz, G. W. Flynn, and R. E. Weston, Jr., "Translationally and Rotationally Resolved Excitation of $CO_2(00^02)$ by Collisions with Hot Hydrogen Atoms," submitted for publication.

J. J. Breen, G. W. Flynn, K. J. Kilgore, and M. T. Jones, "STM Studies of an Organic Conductor Formed from DMTTT and TCNQ," submitted for publication.

J. J. Breen, J. S. Tolman, and G. W. Flynn, "STM Studies of Vapor Deposited Films of TTF and Iodine," submitted for publication.

J. A. Tuchman, Z. Sui, S. Kim, and I. P. Herman, "Photoluminescence of ZnSe/ZnMnSe Superlattices under Hydrostatic Pressure"submitted for publication.

J. A. Tuchman, Z. Sui, S. Kim, and I. P. Herman, "Exciton Photoluminescence in Strained and Unstrained ZnSe under Hydrostatic Pressure"submitted for publication.

Q. Y. Ma, M. T. Schmidt, E. S. Yang, S.-W. Chan, D. Bhattachayra, J. P. Zheng, and H. S. Kwok, "Al/Au and Cu/Au Bilayer-Metal Contacts to YBCO Thin Films," Appl. Phys. Lett., submitted.